

AD-A064 311

DOUGLAS AIRCRAFT CO LONG BEACH CALIF
STUDIES ON THREE-DIMENSIONAL BOUNDARY LAYERS ON BODIES OF REVOL--ETC(U)
AUG 78 T CEBECI, A K KHATTAB, K STEWARTSON

N60921-77-C-0096

NL

UNCLASSIFIED

MDC-J7985

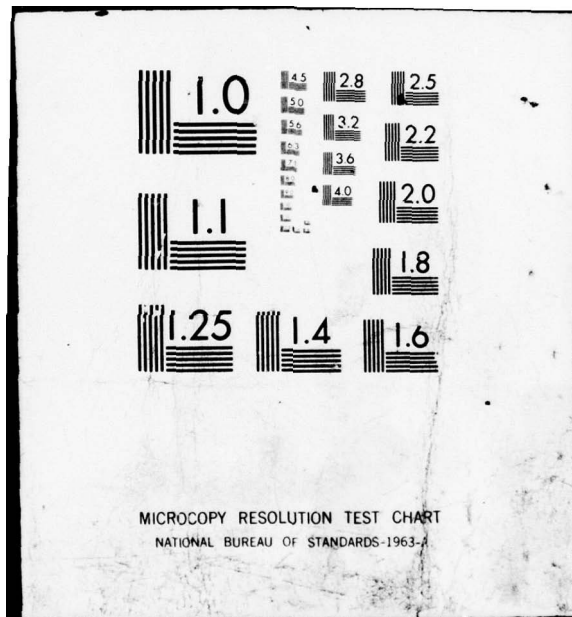
F/G 20/4

| OF |
AD
AO 64 311



END
DATE
FILMED

4 --79
DDC



ADA 064311

DOC FILE COPY

~~LEWIS~~ APPROVED
1
STUDIES ON THREE-DIMENSIONAL BOUNDARY
LAYERS ON BODIES OF REVOLUTION

I. NOSE SEPARATION

by

Tuncer Cebeci, A. K. Khattab and Keith Stewartson

August 1978

Contract No. N60921-77-C-0095

DOUGLAS AIRCRAFT COMPANY

MCDONNELL DOUGLAS

CORPORATION

Equations (2.10) to (2.12) then can be written as

x-Momentum

(11) Report No. JDC J7985

STUDIES ON THREE-DIMENSIONAL BOUNDARY LAYERS
ON BODIES OF REVOLUTION

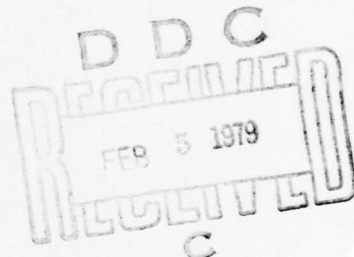
I. NOSE SEPARATION

M See P473

by

Tuncer Cebeci, A. K. Khattab and Keith Stewartson

August 1978



Contract No. N60921-77-C-0096

for

Naval Surface Weapons Center
White Oak Laboratory
Silver Spring, Md. 20910

Approved for public release; distribution unlimited

79 01 31 013

Copy number

Report number

MDC J7985

STUDIES ON THREE-DIMENSIONAL BOUNDARY LAYERS
ON BODIES OF REVOLUTION

I. NOSE SEPARATION

Revision date

Revision letter

Issue date August 1978

Contract number N60921-77-C-0096

Prepared by : Tuncer Cebeci, A. K. Khattab and Keith Stewartson

Approved by :

F. T. Lynch

F. T. Lynch, Branch Chief
Research and Development
Aerodynamics Subdivision

R. B. Harris

R. B. Harris
Chief Technology Engineer
Aerodynamics

ACCESSORY	REPRODUCTION	<input checked="" type="checkbox"/>
NTIS	DATA SHEET	<input type="checkbox"/>
DDO	DATA SHEET	<input type="checkbox"/>
TRANSLATION	DATA SHEET	<input type="checkbox"/>
JOURNAL	DATA SHEET	<input type="checkbox"/>
DISSEMINATION RIGHTS CODES		
SPECIAL		
X		

DOUGLAS AIRCRAFT COMPANY

MCDONNELL DOUGLAS

CORPORATION

TABLE OF CONTENTS

I.	Introduction	1
II.	Formulation for Prolate Spheroids	3
2.1	Basic Equations	3
2.2	Nose Region Coordinates	5
2.3	Line of Symmetry Transformations	8
III.	Formulation for Slender Prolate Spheroids	11
IV.	Numerical Method	16
4.1	Solution of the Line of Symmetry Equations: Finite-Thickness Case	16
4.2	Solution of the Line of Symmetry Equations: "Zero"-Thickness Case	21
V.	Results	23
5.1	Asymptotic Theory for Zero-Thickness Case	23
5.2	The Two-Dimensional Airfoil	26
5.3	Numerical Results for the Line of Symmetry Flow	29
VI.	Discussion	36
VII.	References	39

LIST OF FIGURES

<u>No.</u>	<u>Title</u>	<u>Page</u>
1	Notation for prolate spheroid at incidence	3
2	Finite-difference notation for the Box scheme	17
3	Variation of u_e with X for $\beta = 0.9$	28
4	Variation of separation point with β	29
5	Variation of the longitudinal component of wall shear, $U'(0)$ for paraboloids of zero thickness ratio with p for various α . The dashed lines indicate the asymptotic results for $\alpha = 30^\circ$. .	30
6	Variation of the transverse component of wall shear $W(0)$ for paraboloids of zero thickness ratio with p for various α . The dashed lines indicate the asymptotic results for $\alpha = 30^\circ$. .	31
7	The variation of separation point p_s on paraboloids of zero thickness ratio with α	32
8	The profiles of the cross-flow velocity w at $\alpha = 30^\circ$ for various values of p : - o - o - o are the asymptotic forms, windward to the right and leeward to the left. The dependence of w on Z/X has been scaled out	33
9	The variation of Δ_1 , Δ_2 for paraboloids of zero thickness with p for $\alpha = 30^\circ$. The dashed lines are the asymptotic results	34
10	The variation of the longitudinal local skin-friction coefficient, c_f , with axial distance from the nose ($x = -1$) for a para- boloid of thickness ratio 1/4 and various angles of incidence .	35
11	Sketch of open separation	36

I. INTRODUCTION

This report describes one phase of the work done towards the development of a general boundary-layer method for calculating three-dimensional boundary layers on bodies of revolution at incidence. In this report we address ourselves to the problem of computing boundary layers near the nose region and with the onset of leading-edge separation; this is important for the calculation of transition by stability theory and for the prediction of downstream flow properties including possible separation.

It is well known that separation bubbles can develop near the forward stagnation point of a thin, two-dimensional, plane airfoil at quite small incidences. This phenomenon was first described by Jones¹ and later Gault² carried out an extensive experimental study. Once separation occurs some new features of the flow occur, including long and short bubbles, transition to turbulence and bursting. A review of the developments has been written by Tani³ and later Gaster⁴ reinforced Gault's conclusion that when separation takes place a noticeable interaction takes place between the boundary layer and the mainstream. The theoretical treatment of the interaction is of special interest to aerodynamicists and an important contribution has been made by Briley and McDonald⁵ who interacted the boundary-layer and inviscid equations over the majority of the flow field but used the full Navier-Stokes equations in the neighborhood of separation. By these means they were able to avoid the Goldstein singularity⁶ which is an inevitable feature of classical boundary-layer theory at separation when the pressure gradient is prescribed. We are interested, in this report, in the problem of leading-edge separation from a rational standpoint in which it seems likely that the angle of incidence, that just provokes separation, tends to zero with the thickness ratio t of the airfoil. Further it appears that while the boundary-layer assumption remains true so long as separation does not occur, once it does the singularity inevitably appears. The correct limiting solution, as the Reynolds number based on the leading-edge radius leads to infinity, is then of a different form and most likely given by the Kirchhoff-Sychev theory⁷ in which a free streamline springs from the airfoil at the maximum slip-velocity on the airfoil and may never reattach. The present study is concerned mainly with determining the boundary-layer properties when separation does not occur and to finding the critical angle of incidence which just provokes separation.

The corresponding problem for bodies of revolution has received less attention but there have been a number of important studies by Wang on the laminar boundary layers on prolate bodies of revolution which have an important bearing and to which we shall refer in detail throughout this report. The results of his researches are summarized in a recent review⁸. For example, he has shown^{9,10} that, for the thickness ratio $t = 1/4$, separation on the leeside of the line of symmetry occurs near the rear of the body for angles of incidence $\alpha < 40^\circ$ but that at larger values of α a new separation develops very near the nose. The reason is essentially similar to that for two-dimensional flows, being due to the high curvature of the nose. There is a local velocity overshoot followed immediately afterwards by a short adverse pressure gradient as the main stream returns to a value approximately equal to that at an infinite distance upstream. If this gradient is insufficient to provoke separation, then the boundary layer continues to develop smoothly until, near the rear stagnation point, it encounters a sufficiently severe gradient to compel it to separate. Otherwise the boundary layer breaks down near the nose and as in two dimensions no further progress appears to be possible on a rational theory. It may well be that a freestream surface then springs off the body but there is much less certainty than in two dimensions about the flow properties once classical theory breaks down.

The remainder of the present report has been prepared in five sections. The equations appropriate to prolate spheroids are considered in the following section and for thin prolate spheroids in Chapter III: a coordinate system appropriate to the nose region and transformations appropriate to the line of symmetry are considered in subsections of Chapter II. Solution procedures are considered in Chapter IV where particular attention is devoted to the "line of symmetry" equations for the finite- and zero-thickness cases. Results are presented in Chapter V and discussed in Chapter VI.

II. FORMULATION FOR PROLATE SPHEROIDS

2.1 Basic Equations

For a prolate spheroid at incidence (see Fig. 1), the governing boundary-layer equations for an incompressible laminar flow in a curvilinear orthogonal coordinate system are given by the following equations:

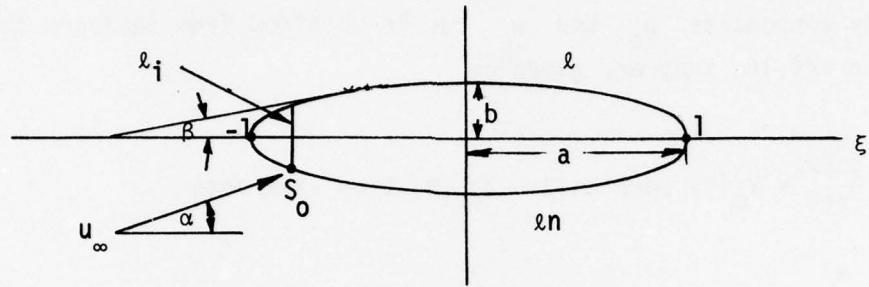


Figure 1. Notation for prolate spheroid at incidence.

Continuity

$$\frac{\partial}{\partial x} (h_2 u) + \frac{\partial}{\partial \theta} (h_1 w) + \frac{\partial}{\partial y} (h_1 h_2 v) = 0 \quad (2.1)$$

x -Momentum

$$\frac{u}{h_1} \frac{\partial u}{\partial x} + \frac{w}{h_2} \frac{\partial u}{\partial \theta} + v \frac{\partial u}{\partial y} + w^2 K_2 = - \frac{1}{\rho h_1} \frac{\partial p}{\partial x} + v \frac{\partial^2 u}{\partial y^2} \quad (2.2)$$

θ -Momentum

$$\frac{u}{h_1} \frac{\partial w}{\partial x} + \frac{w}{h_2} \frac{\partial w}{\partial \theta} + v \frac{\partial w}{\partial y} - uwK_2 = - \frac{1}{\rho h_2} \frac{\partial p}{\partial \theta} + v \frac{\partial^2 w}{\partial y^2} \quad (2.3)$$

Here h_1, h_2 are metric coefficients defined by

$$h_1 = \left[\frac{1 + \xi^2(t^2 - 1)}{1 - \xi^2} \right]^{1/2} \quad h_2 = t(1 - \xi^2)^{1/2} \quad (2.4)$$

where t denotes the thickness ratio ($=b/a$) of the elliptic profile. The parameter K_2 is the geodesic curvature of the surface lines $\xi (=x/a) = \text{const.}$ and is given by

$$K_2 = \frac{t\xi}{h_1 h_2 (1 - \xi^2)^{1/2}} \quad (2.5)$$

The solution of the system (2.1) to (2.5) requires boundary conditions and initial conditions. The boundary conditions are:

$$y = 0, \quad u = v = w = 0; \quad y \rightarrow \infty, \quad u \rightarrow u_e(x, \theta), \quad w \rightarrow w_e(x, \theta) \quad (2.6)$$

The velocity components u_e and w_e can be obtained from inviscid theory. According to ref.14, they are given by

$$\frac{u_e}{u_{\text{ref}}} = V_0(t) \cos\alpha \cos\beta - V_{90}(t) \sin\alpha \sin\beta \cos\theta \quad (2.7a)$$

$$\frac{w_e}{u_{\text{ref}}} = V_{90}(t) \sin\alpha \sin\theta \quad (2.7b)$$

Here β denotes the angle between the line tangent to the elliptic profile and the positive ξ -axis. It is given by

$$\cos\beta = \frac{(1 - \xi^2)^{1/2}}{[1 + \xi^2(t^2 - 1)]^{1/2}} \quad (2.8)$$

The parameters $V_0(t)$ and $V_{90}(t)$ are functions of t , defined by

$$V_0(t) = \frac{(1 - t^2)^{3/2}}{\sqrt{(1 - t^2) - t^2/2} \ln \left\{ [1 + (1 - t^2)^{1/2}] / [1 - (1 - t^2)^{1/2}] \right\}} \quad (2.9a)$$

$$V_{90}(t) = \frac{2V_0(t)}{2V_0(t) - 1} \quad (2.9b)$$

The initial conditions in the longitudinal direction can be calculated by taking advantage of the symmetry conditions. Noting that the circumferential velocity in the boundary layer and the circumferential pressure gradient are identically zero on the line of symmetry, we differentiate this equation with respect to θ to obtain the so-called attachment-line equations in the longitudinal direction:

Continuity

$$\frac{\partial}{\partial x} (h_2 u) + h_1 w_\theta + \frac{\partial}{\partial y} (h_1 h_2 v) = 0 \quad (2.10)$$

x-Momentum

$$\frac{u}{h_1} \frac{\partial u}{\partial x} + v \frac{\partial u}{\partial y} = - \frac{1}{\rho h_1} \frac{\partial p}{\partial x} + v \frac{\partial^2 u}{\partial y^2} \quad (2.11)$$

θ -Momentum

$$\frac{u}{h_1} \frac{\partial w_\theta}{\partial x} + \frac{w_\theta^2}{h_2} + v \frac{\partial w_\theta}{\partial y} - uw_\theta K_2 = - \frac{1}{\rho h_2} \frac{\partial^2 p}{\partial \theta^2} + v \frac{\partial^2 w_\theta}{\partial y^2} \quad (2.12)$$

where $w_\theta = \partial w / \partial \theta$. These equations are subject to the boundary conditions:

$$y = 0, \quad u, v, w = 0; \quad y \rightarrow \infty \quad u \rightarrow u_e, \quad w \rightarrow w_{\theta e} \quad (2.13)$$

The specification of the initial conditions in the circumferential direction is not quite so easy when body-oriented coordinates are used because of the singularity in the properties of h_1 , h_2 and K_2 at the nose ($x = -1$). A common approach used to circumvent this unpleasant geometric singularity is to revert to an approximate procedure by first performing the integration along the line of symmetry from the stagnation point as near to the nose as possible, then jumping around the body along the line ℓ_i to the same value of x on the leeward side ($\theta = \pi$) as shown in Fig. 1. Afterwards the solution may be extended to more general points on the body. Such a procedure, while effective at moderate values of α and/or t leads to difficulties and to inaccuracies as α increases and $t \rightarrow 0$. These difficulties can be circumvented as described in sections 2.2 and in Chapter III.

2.2 Nose Region Coordinates

The difficulties and inaccuracies associated with generating initial conditions caused by the singularities due to h_1 , h_2 and K_2 in the circumferential direction can be avoided by using a suitable transformation near $x = -1$. We define new velocity components U , W , V by

$$u = U \cos \theta + W \sin \theta \quad (2.14a)$$

$$w = W \cos\theta - U \sin\theta \quad (2.14b)$$

$$v = V/t \quad (2.14c)$$

and new coordinates X, Y, Z by

$$X = S \cos\theta \quad (2.15a)$$

$$Z = S \sin\theta \quad (2.15b)$$

$$Y = v/t \quad (2.15c)$$

Here S is a parameter which is a function of x , only, and defined in (2.20) below.

The purpose of the above transformation is to convert the polar form of the equations (2.1) to (2.3) near the nose into a quasi-rectangular Cartesian form which is free of singularities. The basic reasoning behind this transformation can be appreciated by noting the advantages of solving the Laplacian near the origin in the form

$$\frac{\partial^2}{\partial x^2} + \frac{\partial^2}{\partial y^2}$$

compared with

$$\frac{\partial^2}{\partial r^2} + \frac{1}{r} \frac{\partial}{\partial r} + \frac{1}{r^2} \frac{\partial^2}{\partial \theta^2}$$

By means of this transformation it can be shown, after considerable algebra, that equations (2.1) to (2.3) reduce to

Continuity

$$N \left(\frac{\partial U}{\partial X} + \frac{\partial W}{\partial Z} \right) + \frac{\partial V}{\partial Y} - L(UX + WZ) = 0 \quad (2.16)$$

X-Momentum

$$N \left(U \frac{\partial U}{\partial X} + W \frac{\partial U}{\partial Z} \right) + LW(WX - UZ) + V \frac{\partial U}{\partial Y} = \tilde{\beta}_1 + v \frac{\partial^2 U}{\partial Y^2} \quad (2.17)$$

Z-Momentum

$$N \left(U \frac{\partial W}{\partial X} + W \frac{\partial W}{\partial Z} \right) - LU(WX - UZ) + V \frac{\partial W}{\partial Y} = \tilde{\beta}_2 + v \frac{\partial^2 W}{\partial Y^2} \quad (2.18)$$

Here $\tilde{\beta}_1$ and $\tilde{\beta}_2$ are pressure-gradient parameters defined by

$$\tilde{\beta}_1 = N \left(U_e \frac{\partial U_e}{\partial X} + W_e \frac{\partial U_e}{\partial Z} \right) + L W_e (W_e X - U_e Z) \quad (2.19a)$$

$$\tilde{\beta}_2 = N \left(U_e \frac{\partial W_e}{\partial X} + W_e \frac{\partial W_e}{\partial Z} \right) - L U_e (W_e X - U_e Z) \quad (2.19b)$$

The function S is obtained by integrating the expression

$$\frac{dS}{S} = \frac{[1 + \xi^2(t^2 - 1)]^{1/2}}{t(1 - \xi^2)} d\xi \quad (2.20)$$

subject to $S = 0$ at $\xi = -1$, and

$$N = \frac{St^2}{h_2}, \quad L = \frac{t^2}{S} \left(\frac{1}{h_2} + K_2 \right) \quad (2.21)$$

Along the line of symmetry, (2.16) to (2.18) become:

Continuity:

$$N \left(\frac{\partial U}{\partial X} + W_Z \right) + \frac{\partial V}{\partial Y} - LUX = 0 \quad (2.22)$$

X-Momentum

$$NU \frac{\partial U}{\partial X} + V \frac{\partial U}{\partial Y} = \beta_1^* + v \frac{\partial^2 U}{\partial Y^2} \quad (2.23)$$

Z-Momentum

$$N \left(U \frac{\partial W_Z}{\partial X} + W_Z^2 \right) - LU(W_Z X - U) + V \frac{\partial W_Z}{\partial Y} = \beta_2^* + v \frac{\partial^2 W_Z}{\partial Y^2} \quad (2.24)$$

where W_Z denotes $\partial W / \partial Z$ and the pressure-gradient parameters β_1^* and β_2^* are now

$$\beta_1^* = NU_e \frac{\partial U_e}{\partial X}, \quad \beta_2^* = N \left(U_e \frac{\partial W_{Ze}}{\partial X} + W_{Ze}^2 \right) - LU_e (W_{Ze} X - U_e) \quad (2.25)$$

The appropriate boundary conditions are:

$$Y = 0, \quad U = V = W_Z = 0; \quad Y \rightarrow \infty, \quad U \rightarrow U_e(X), \quad W_Z \rightarrow W_{Ze}(X) \quad (2.26)$$

At the stagnation point S_0 , where both U and W are zero, the governing equations (2.22) to (2.24) and their boundary conditions (2.26) reduce to:

Continuity

$$N(U_X + W_Z) + V_Y = 0 \quad (2.27)$$

X-Momentum

$$NU_X^2 + V \frac{\partial U_X}{\partial Y} = \beta_1^{**} + v \frac{\partial^2 U_X}{\partial Y^2} \quad (2.28)$$

Z-Momentum

$$NW_Z^2 + V \frac{\partial W_Z}{\partial Y} = \beta_2^{**} + v \frac{\partial^2 W_Z}{\partial Y^2} \quad (2.29)$$

$$Y = 0, \quad U_X = V = W_Z = 0; \quad Y \rightarrow \infty, \quad U_X \rightarrow U_{Xe}, \quad W_Z \rightarrow W_{Ze} \quad (2.30)$$

In (2.28) and (2.29), the pressure gradient parameters β_1^{**} and β_2^{**} are

$$\beta_1^{**} = NU_{Xe}^2, \quad \beta_2^{**} = NW_{Ze}^2 \quad (2.31)$$

2.3 Line of Symmetry Transformations

To solve the line of symmetry equations, we find it convenient to use a transformation which we employed in our previous studies. For the nose-region equations given by (2.22), (2.23), (2.24) and (2.26), we let

$$\eta^* = \sqrt{\frac{U_{ref}}{vC}} Y \quad (2.32)$$

and introduce a two-component vector potential such that

$$U = \frac{\partial \psi}{\partial Y}, \quad W_Z = \frac{\partial \phi}{\partial Y}, \quad V = - \left(N \frac{\partial \psi}{\partial X} + N\phi - L\psi X \right) \quad (2.33)$$

In addition, we define dimensionless ψ and ϕ by

$$\psi = \sqrt{U_{ref} v C} F(X, \eta^*) \quad (2.34a)$$

$$\phi = \sqrt{U_{ref} v C} G(X, \eta^*) \quad (2.34b)$$

Here U_{ref} and c are respectively a reference velocity and length introduced for convenience of comparison with Ref. 14; both are unity throughout this paper. The line of symmetry equations for the nose region may now be written as

X-Momentum

$$F''' + F''(NG - LFX) = N \left(F' \frac{\partial F'}{\partial X} - F'' \frac{\partial F}{\partial X} \right) - \beta_1^* \quad (2.35)$$

Z-Momentum

$$G''' - N(G')^2 + LF'(G'X - F') + G''(NG - LFX) = N \left(F' \frac{\partial G'}{\partial X} - G'' \frac{\partial F}{\partial X} \right) - \beta_2^* \quad (2.36)$$

Here primes denote differentiation with respect to η^* and

$$F' = \frac{U}{U_{ref}}, \quad G' = \frac{W_Z}{U_{ref}} \quad (2.37)$$

The boundary conditions (2.26) become

$$\eta^* = 0, \quad F = F' = G = G' = 0; \quad \eta^* \rightarrow \infty, \quad F' \rightarrow \frac{U_e}{U_{ref}}, \quad G' = \frac{W_Z}{U_{ref}} \quad (2.38)$$

At some distance away from the nose, we also find it more convenient to express the governing equations (2.10) to (2.13) in terms of new variables defined by

$$\eta = \sqrt{\frac{U_{ref}}{vs_1}} y \quad (2.39a)$$

where s_1 is the arc length along the x-coordinate given by

$$s_1 = \int_{-1}^x h_1 dx \quad (2.39b)$$

Again we introduce a two-component vector potential that satisfies the continuity equation (2.10),

$$uh_2 = \frac{\partial \tilde{\psi}}{\partial y}, \quad w_\theta h_1 = \frac{\partial \tilde{\phi}}{\partial y}, \quad vh_1 h_2 = - \left(\frac{\partial \tilde{\psi}}{\partial x} + \tilde{\phi} \right) \quad (2.40a)$$

together with dimensionless $\tilde{\psi}$ and $\tilde{\phi}$ given by

$$\tilde{\psi} = \sqrt{U_{ref} vs_1} h_2 f(x, \eta) \quad \tilde{\phi} = \sqrt{U_{ref} vs_1} h_1 g(x, \eta) \quad (2.40b)$$

Equations (2.10) to (2.12) then can be written as

x-Momentum

$$f''' + m_1 f f'' + m_2 f'' g + m_6 = m_7 \left(f' \frac{\partial f'}{\partial x} - f'' \frac{\partial f}{\partial x} \right) \quad (2.41)$$

z-Momentum

$$g''' + m_1 f g'' + m_2 g g'' + m_3 f' g' - m_4 (g')^2 + m_5 = m_7 \left(f' \frac{\partial g'}{\partial x} - g'' \frac{\partial f}{\partial x} \right) \quad (2.42)$$

Here primes denote differentiation with respect to η , and the quantities m_1, \dots, m_7 denote the dimensionless parameters:

$$\begin{aligned} m_1 &= \frac{1}{2} - s_1 k_2, & m_2 &= \frac{s_1}{h_2}, & m_3 &= s_1 k_2 \\ m_4 &= m_2, & m_5 &= \frac{s_1}{U_{ref}^2} \left(\frac{u_e}{h_1} \frac{\partial w_{\theta e}}{\partial x} + \frac{w_{\theta e}^2}{h_2} - k_2 u_e w_{\theta e} \right) \\ m_6 &= \frac{s_1}{U_{ref}^2} \frac{u_e}{h_1} \frac{\partial u_e}{\partial x}, & m_7 &= \frac{s_1}{h_1} \end{aligned} \quad (2.43)$$

Also

$$f' = \frac{u}{U_{ref}}, \quad g' = \frac{w_{\theta e}}{U_{ref}} \quad (2.44)$$

The boundary conditions become:

$$\eta = 0, \quad f = f' = g = g' = 0; \quad \eta \rightarrow \infty, \quad f' \rightarrow \frac{u_e}{U_{ref}}, \quad g' = \frac{w_{\theta e}}{U_{ref}} \quad (2.45)$$

III. FORMULATION FOR SLENDER PROLATE SPHEROIDS

As we shall see later, it is desirable and convenient to study the boundary layers on very slender prolate spheroids, i.e., $t \rightarrow 0$. To obtain the governing equations appropriate for such bodies, we use the coordinates (2.14) and (2.15) and define

$$p = \frac{\sqrt{1 - x^2}}{t} \quad (3.1)$$

Then we take the limit $t \rightarrow 0$, holding p and S finite. Again after a considerable algebra, we obtain the following equations:

Continuity:

$$N \left(\frac{\partial U}{\partial X} + \frac{\partial W}{\partial Z} \right) + \frac{\partial V}{\partial Y} - L (UX + WZ) = 0 \quad (3.2)$$

X-Momentum

$$N \left(U \frac{\partial U}{\partial X} + W \frac{\partial U}{\partial Z} \right) + V \frac{\partial U}{\partial Y} - LW(WX - UZ) = \tilde{\beta}_1 + v \frac{\partial^2 U}{\partial Y^2} \quad (3.3)$$

Z-Momentum

$$N \left(U \frac{\partial W}{\partial X} + W \frac{\partial W}{\partial Z} \right) + V \frac{\partial W}{\partial Y} - LU(WX - UZ) = \tilde{\beta}_2 + v \frac{\partial^2 W}{\partial Y^2} \quad (3.4)$$

Here

$$S = \frac{p}{(1 + p^2)^{1/2} + 1} \exp[\sqrt{1 + p^2} - 1], \quad (3.5a)$$

$$N = \frac{S}{p}, \quad L = \frac{\sqrt{1 + p^2} - 1}{pS\sqrt{1 + p^2}}, \quad (3.5b)$$

$$\tilde{\beta}_1 = N \left(U_e \frac{\partial U_e}{\partial X} + W_e \frac{\partial U_e}{\partial Z} \right) + LW_e(W_e X - U_e Z) \quad (3.5c)$$

$$\tilde{\beta}_2 = N \left(U_e \frac{\partial W_e}{\partial X} + W_e \frac{\partial W_e}{\partial Z} \right) - LU_e(W_e X - U_e Z) \quad (3.5d)$$

and U_e is the limit as $t \rightarrow 0$ of $u_e \cos\theta + w_e \sin\theta$, i.e.

$$U_e = \frac{px \cos \alpha}{s\sqrt{1+p^2}} - 2 \left(1 - \frac{px^2 L}{s}\right) \sin \alpha \quad (3.5e)$$

Similarly,

$$W_e = \frac{pz \cos \alpha}{s\sqrt{1+p^2}} + \frac{2xzLp}{s} \sin \alpha \quad (3.5f)$$

The boundary conditions satisfied by U , W , V are:

$$\begin{aligned} Y = 0, \quad U = V = W = 0; \\ Y \rightarrow \infty, \quad U \rightarrow U_e, \quad W \rightarrow W_e \end{aligned} \quad (3.6)$$

These equations are explicitly independent of t and moreover are free of singularities at $p = 0$. It can be expected therefore that the solution is also quite smooth and in particular at the nose, now defined by $X = Z = 0$ the numerical integration present no difficulties. It is interesting to note from (3.5a) that a finite value of S corresponds to a finite value of p , with $S/p \rightarrow 1$ as $p \rightarrow 0$, and hence from (3.1) to a distance from the nose $O(t^2)$. The set of equations (3.2), (3.3), (3.4) is appropriate therefore within a distance from the nose of general axisymmetric thin smooth bodies of the order of the radius of curvature there.

To obtain the line of symmetry equations for the system given by (3.2) through (3.4) and (3.6), we define

$$U = U_0(X, Y) + O(z^2) \quad (3.7a)$$

$$V = V_0(X, Y) + O(z^2) \quad (3.7b)$$

$$W = Z \exp(1 - \sqrt{1+p^2}) W_1(X, Y) + O(z^3) \quad (3.7c)$$

We allow for negative values of X by permitting p to take negative values. When $p < 0$, the sign of S in (3.5a) must be changed and generally $X = S \operatorname{sgn} p$ in the limit $Z \rightarrow 0$. Near the line of symmetry the longitudinal and transverse components of velocity in the boundary layer are

$$u = U_0 \operatorname{sgn} p + O(z^2) \quad (3.8a)$$

and

$$w = \frac{Z}{S} \left(\frac{pw_1}{1 + \sqrt{1+p^2}} - U_0 \right) + O(z^3) \quad (3.8b)$$

respectively. We now substitute (3.7) into (3.2) to (3.4) and take the limit $Z \rightarrow 0$, obtaining the equations

Continuity:

$$\frac{\partial U_0}{\partial p} + \frac{\sqrt{1+p^2}}{\sqrt{1+p^2+1}} W_1 + \sqrt{1+p^2} \frac{\partial V_0}{\partial Y} - \left(\frac{p}{\sqrt{p^2+1+1}} \right) U_0 = 0 \quad (3.9)$$

X-Momentum

$$\frac{U_0}{\sqrt{1+p^2}} \frac{\partial U_0}{\partial p} + V_0 \frac{\partial U_0}{\partial Y} = \beta_1^* + v \frac{\partial^2 U_0}{\partial Y^2} \quad (3.10)$$

Z-Momentum

$$\frac{U_0}{\sqrt{1+p^2}} \frac{\partial W_1}{\partial p} + V_0 \frac{\partial W_1}{\partial Y} + \frac{U_0^2}{\sqrt{1+p^2}} + \frac{W_1^2}{1+\sqrt{1+p^2}} - \Lambda_0 U_0 W_1 = \beta_2^* + v \frac{\partial^2 W_1}{\partial Y^2} \quad (3.11)$$

with boundary conditions

$$Y = 0, \quad U_0 = V_0 = W_1 = 0 \quad (3.12)$$

$$Y \rightarrow \infty \quad U_0 \rightarrow U_{oe} \quad W_1 \rightarrow W_{1e}$$

Here

$$\beta_1^* = \frac{U_{oe}}{\sqrt{1+p^2}} \frac{\partial U_{oe}}{\partial p} \quad (3.13a)$$

$$\beta_2^* = \frac{U_{oe}}{\sqrt{1+p^2}} \frac{\partial W_{1e}}{\partial p} + \frac{U_{oe}^2}{\sqrt{1+p^2}} - U_{oe} W_{1e} \Lambda_0 + \frac{W_{1e}^2}{1+\sqrt{1+p^2}} \quad (3.13b)$$

$$\Lambda_0 = \frac{p}{1+p^2} + \frac{p}{1+p^2+\sqrt{1+p^2}} \quad (3.13b)$$

and

$$U_{oe} = \frac{p \cos\alpha - 2 \sin\alpha}{\sqrt{1 + p^2}} \quad (3.14a)$$

$$W_{le} = \frac{(\sqrt{1 + p^2} + 1) \cos\alpha + 2p \sin\alpha}{\sqrt{1 + p^2}} \quad (3.14b)$$

In order to place the above equations into a more convenient form (see Chapter V), we now define n and \bar{V} by

$$n = \frac{\gamma}{(1 + p^2)^{1/4}} \frac{1}{\sqrt{v}} \quad (3.15a)$$

$$\bar{V} = V_0 \frac{(1 + p^2)^{1/4}}{\sqrt{v}} - \frac{npU_0}{2(1 + p^2)} \quad (3.15b)$$

and write the continuity equation (3.9) and the two momentum equations (3.10) and (3.11) as

Continuity

$$\frac{\partial U_0}{\partial p} + \frac{\partial \bar{V}}{\partial n} + a_1 U_0 + a_2 W_1 = 0 \quad (3.16)$$

X-Momentum

$$U_0 \frac{\partial U_0}{\partial p} + \bar{V} \frac{\partial U_0}{\partial n} = \beta_1^* + \frac{\partial^2 U_0}{\partial n^2} \quad (3.17)$$

Z-Momentum

$$U_0 \frac{\partial W_1}{\partial p} - a_3 U_0 W_1 + a_2 W_1^2 + U_0^2 + \bar{V} \frac{\partial W_1}{\partial n} = \beta_2^* + \frac{\partial^2 W_1}{\partial n^2} \quad (3.18)$$

Here a_1 , a_2 and a_3 are functions of p and are given by

$$a_1 = \frac{p}{2(1 + p^2)} - \frac{p}{\sqrt{p^2 + 1} + 1}, \quad a_2 = \frac{\sqrt{1 + p^2}}{\sqrt{1 + p^2} + 1} \quad (3.19)$$

$$a_3 = \frac{p}{\sqrt{1 + p^2}} + \frac{p}{\sqrt{1 + p^2} + 1}$$

The pressure-gradient parameters in (3.17) and (3.18) are

$$\beta_1^* = U_{oe} \frac{\partial U_{oe}}{\partial p}, \quad \beta_2^* = U_{oe}^2 - a_3 U_{oe} W_{1e} + U_{oe} \frac{\partial W_{1e}}{\partial p} + a_2 W_{1e}^2 \quad (3.20)$$

and the boundary conditions (3.12) remain unaffected, except now γ is replaced by η . At the stagnation point, (3.16), (3.17) and (3.18) become

Continuity

$$U_1 + \frac{\partial V}{\partial \eta} + a_2 W_1 = 0 \quad (3.21)$$

X-Momentum

$$U_1^2 + \bar{V} \frac{\partial U_1}{\partial \eta} = \beta_1 + v \frac{\partial^2 U_1}{\partial \eta^2} \quad (3.22)$$

Z-Momentum

$$a_2 W_1^2 + \bar{V} \frac{\partial W_1}{\partial \eta} = \beta_2 + v \frac{\partial^2 W_1}{\partial \eta^2} \quad (3.23)$$

where $U_1 = \partial U_0 / \partial p$.

$$\eta = 0, \quad U_1 = \bar{V} = W_1 = 0 \quad (3.24)$$

$$\eta \rightarrow \infty \quad U_1 \rightarrow U_{1e} \quad W \rightarrow W_{1e}$$

The pressure gradient parameters $\tilde{\beta}_1$ and $\tilde{\beta}_2$ are

$$\tilde{\beta}_1 = U_{1e}^2, \quad \tilde{\beta}_2 = a_2 W_{1e}^2 \quad (3.25)$$

and

$$U_{1e} = \frac{\cos \alpha}{\sqrt{1 + p_0^2}}, \quad W_{1e} = \frac{(1 + \sqrt{1 + p_0^2}) \cos \alpha + 2p_0 \sin \alpha}{\sqrt{p_0^2 + 1}} \quad (3.26)$$

with

$$p_0 = 2 \tan \alpha \quad (3.27)$$

IV. NUMERICAL METHOD

We use the Box method to solve the governing equations in Chapters II and III. This is a two-point finite-difference method developed by Keller and Cebeci. This method has been applied to two-dimensional flows as well as three-dimensional flows and has been found to be efficient and accurate. Descriptions of this method have been presented in a series of papers and reports and a detailed presentation is contained in a recent book by Cebeci and Bradshaw¹¹. Therefore, only a brief description of it is presented below.

4.1 Solution of the Line of Symmetry Equations: Finite-Thickness Case

According to the Box method, we first reduce the equations (2.35) to (2.36) into a system of first-order equations. The system (2.35) to (2.36) can either be expressed as five first-order equations or as six first-order equations. For the line-of-symmetry equations, there is little advantage (if any) between either choice. However, to get the solutions off the line of symmetry, the choice of five first-order equations appears to be more convenient and more suitable for our numerical work. In our study we decided to consider both choices. Here we shall describe the solution procedure for the finite-thickness case when the system (2.35) to (2.36) is reduced to a system of six first-order equations by introducing new dependent variables $U(X, \eta^*)$, $V(X, \eta^*)$, $W(X, \eta^*)$ and $T(X, \eta^*)$

$$F' = U \quad (4.1a)$$

$$U' = V \quad (4.1b)$$

$$G' = W \quad (4.1c)$$

$$W' = T \quad (4.1d)$$

$$V' + V(NG - LFX) + \tilde{\beta}_1 = N\left(U \frac{\partial U}{\partial X} - V \frac{\partial F}{\partial X}\right) \quad (4.1e)$$

$$T' - NW^2 + LU(WX - U) + T(NG - LFX) + \tilde{\beta}_2 = N\left(U \frac{\partial W}{\partial X} - T \frac{\partial F}{\partial X}\right) \quad (4.1f)$$

To solve the system (4.1) subject to

$$\eta^* = 0, \quad F = U = G = W = 0; \quad \eta^* \rightarrow \infty, \quad U = \frac{U_e}{U_{ref}}, \quad W = \frac{W_Z}{U_{ref}} \quad (4.2)$$

we first write finite-difference equations by considering one mesh rectangle

^fFor convenience in referencing earlier papers or the box method we use in this chapter a notation consistent with them. A partial reconciliation with that of the remainder of this paper can be made by setting $U_{ref} = 1$ but the V used here should not be confused with the V defined in (2.14c).

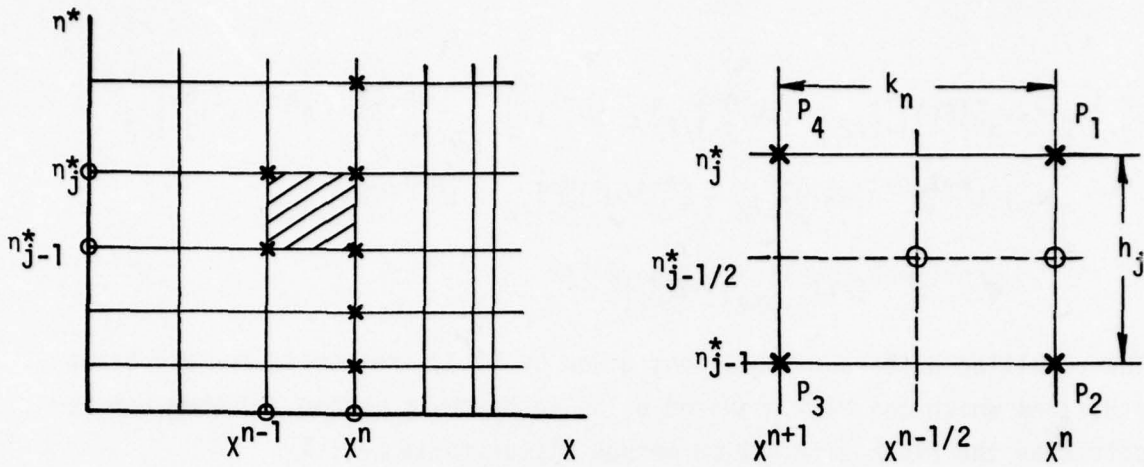


Figure 2. Finite-difference notation for the Box scheme.

as shown in Fig. 2. We approximate (4.1a,b,c,d) using centered difference quotients, average them about the midpoint $(X_n, n_{j-1/2}^*)$ of the segment P_1P_2 , and approximate (4.1e,f) by centering them about the midpoint $(X_{n-1/2}, n_{j-1/2}^*)$ of the rectangle $P_1P_2P_3P_4$. They are given below

$$h_j^{-1}(F_j^n - F_{j-1}^n) = U_{j-1/2}^n \quad (4.3a)$$

$$h_j^{-1}(U_j^n - U_{j-1}^n) = V_{j-1/2}^n \quad (4.3b)$$

$$h_j^{-1}(G_j^n - G_{j-1}^n) = W_{j-1/2}^n \quad (4.3c)$$

$$h_j^{-1}(W_j^n - W_{j-1}^n) = T_{j-1/2}^n \quad (4.3d)$$

$$\begin{aligned} h_j^{-1}(V_j^n - V_{j-1}^n) + N^n(GV)_{j-1/2}^n - L^n X_j^n (FV)_{j-1/2}^n - \alpha_n [(U^2)_{j-1/2}^n - (FV)_{j-1/2}^n] \\ + F_{j-1/2}^{n-1} V_{j-1/2}^n - V_{j-1/2}^{n-1} F_{j-1/2}^n] = R_{j-1/2}^{n-1} \end{aligned} \quad (4.3e)$$

$$\begin{aligned} h_j^{-1}(T_j^n - T_{j-1}^n) - N^n(W^2)_{j-1/2}^n + (L^n X_j^n - \alpha_n)(UW)_{j-1/2}^n - L^n(U^2)_{j-1/2}^n + N^n(GT)_{j-1/2}^n \\ + (\alpha_n - L^n X_j^n)(FT)_{j-1/2}^n - \alpha_n [-W_{j-1/2}^{n-1} U_{j-1/2}^n + U_{j-1/2}^{n-1} W_{j-1/2}^n] \\ + F_{j-1/2}^{n-1} T_{j-1/2}^n - T_{j-1/2}^{n-1} F_{j-1/2}^n] = S_{j-1/2}^{n-1} \end{aligned} \quad (4.3f)$$

where with $\alpha_n = (N^{n-1/2}) / (X_n - X_{n-1}) = N^{n-1/2} k_n^{-1}$

$$\begin{aligned} R_{j-1/2}^{n-1} = \alpha_n [(FV)_{j-1/2}^{n-1} - (U^2)_{j-1/2}^{n-1}] - [h_j^{-1}(V_j^{n-1} - V_{j-1}^{n-1}) + N^{n-1}(GV)_{j-1/2}^{n-1}] \\ - L^{n-1} X_j^{n-1} (FV)_{j-1/2}^{n-1} - 2(\beta_1)^{n-1/2} \end{aligned}$$

$$\begin{aligned}
S_{j-1/2}^{n-1} = & \alpha_n [(FT)_{j-1/2}^{n-1} - (UW)_{j-1/2}^{n-1}] - [h_j^{-1} (T_j^{n-1} - T_{j-1}^{n-1}) - N^{n-1} (w^2)_{j-1/2}^{n-1}] \\
& + L^{n-1} X^{n-1} (UW)_{j-1/2}^{n-1} - L^{n-1} (U^2)_{j-1/2}^{n-1} + N^{n-1} (GT)_{j-1/2}^{n-1} \\
& - L^{n-1} X^{n-1} (FT)_{j-1/2}^{n-1} - 2(\beta_2)^{n-1/2}
\end{aligned}$$

The resulting difference equations given by (4.3) are nonlinear algebraic equations which can be linearized by using Newton's method and then can be solved by the block elimination method discussed in ref. 11.

The linearized difference equations for (4.3) can be expressed in the following form, with $2 \leq j \leq J$,

$$\delta F_j - \delta F_{j-1} - \frac{h_j}{2} (\delta U_j + \delta U_{j-1}) = (r_5)_{j-1} \quad (4.4a)$$

$$\delta U_j - \delta U_{j-1} - \frac{h_j}{2} (\delta U_j + \delta U_{j-1}) = (r_6)_{j-1} \quad (4.4b)$$

$$\delta G_j - \delta G_{j-1} - \frac{h_j}{2} (\delta W_j + \delta W_{j-1}) = (r_1)_j \quad (4.4c)$$

$$\delta W_j - \delta W_{j-1} - \frac{h_j}{2} (\delta T_j + \delta T_{j-1}) = (r_2)_j \quad (4.4d)$$

$$\begin{aligned}
(S_1)_j \delta V_j + (S_2)_j \delta V_{j-1} + (S_3)_j \delta F_j + (S_4)_j \delta F_{j-1} + (S_5)_j \delta U_j + (S_6)_j \delta U_{j-1} \\
+ (S_7)_j \delta G_j + (S_8)_j \delta G_{j-1} = (r_3)_j
\end{aligned} \quad (4.4e)$$

$$\begin{aligned}
(\beta_1)_j \delta T_j + (\beta_2)_j \delta T_{j-1} + (\beta_3)_j \delta F_j + (\beta_4)_j \delta F_{j-1} + (\beta_5)_j \delta W_j + (\beta_6)_j \delta W_{j-1} \\
+ (\beta_7)_j \delta U_j + (\beta_8)_j \delta U_{j-1} + (\beta_9)_j \delta G_j + (\beta_{10})_j \delta G_{j-1} = (r_4)_j
\end{aligned} \quad (4.4f)$$

Here

$$(S_1)_j = \frac{1}{h_j} + \frac{1}{2} N^n G_j^n - \frac{1}{2} (L^n X^n - \alpha_n) F_j^n - \frac{\alpha_n}{2} F_{j-1/2}^{n-1}$$

$$(S_2)_j = -\frac{1}{h_j} + \frac{1}{2} N^n G_{j-1}^n - \frac{1}{2} (L^n X^n - \alpha_n) F_{j-1}^n - \frac{1}{2} \alpha_n F_{j-1/2}^{n-1}$$

$$(S_3)_j = \frac{1}{2} [(\alpha_n - L^n X^n) V_j^n + \alpha_n V_{j-1/2}^{n-1}]$$

$$(s_4)_j = \frac{1}{2} [(\alpha_n - L^n X^n) V_{j-1}^n + \alpha_n V_{j-1/2}^{n-1}]$$

$$(s_5)_j = -\alpha_n U_j^n$$

$$(s_6)_j = -\alpha_n U_{j-1}^n$$

$$(s_7)_j = \frac{1}{2} N^n V_j^n$$

$$(s_8)_j = \frac{1}{2} N^n V_{j-1}^n$$

$$(\beta_1)_j = \frac{1}{h_j} + \frac{1}{2} (N^n G_j^n - (L^n X^n - \alpha_n) F_j^n - \alpha_n F_{j-1/2}^{n-1})$$

$$(\beta_2)_j = -\frac{1}{h_j} + \frac{1}{2} (N^n G_{j-1}^n - (L^n X^n - \alpha_n) F_{j-1}^n - \alpha_n F_{j-1/2}^{n-1}) \quad (4.5)$$

$$(\beta_3)_j = \frac{1}{2} [(\alpha_n - L^n X^n) T_j^n + \alpha_n T_{j-1/2}^{n-1}]$$

$$(\beta_4)_j = \frac{1}{2} [(\alpha_n - L^n X^n) T_{j-1}^n + \alpha_n T_{j-1/2}^{n-1}]$$

$$(\beta_5)_j = -N^n W_j^n + \frac{1}{2} [(L^n X^n - \alpha_n) U_j^n - \alpha_n U_{j-1/2}^{n-1}]$$

$$(\beta_6)_j = -N^n W_{j-1}^n + \frac{1}{2} [(L^n X^n - \alpha_n) U_{j-1}^n - \alpha_n U_{j-1/2}^{n-1}]$$

$$(\beta_7)_j = -L^n U_j^n + \frac{1}{2} [(L^n X^n - \alpha_n) W_j^n + \alpha_n W_{j-1/2}^{n-1}]$$

$$(\beta_8)_j = -L^n U_{j-1}^n + \frac{1}{2} [(L^n X^n - \alpha_n) W_{j-1}^n + \alpha_n W_{j-1/2}^{n-1}]$$

$$(\beta_9)_j = \frac{1}{2} N^n T_j^n$$

$$(\beta_{10})_j = \frac{1}{2} N^n T_{j-1}^n$$

and

$$(r_1)_j = G_{j-1}^n - G_j^n + h_j^{-1} W_{j-1/2}^n \quad (4.6)$$

$$(r_2)_j = W_{j-1}^n - W_j^n + h_j^{-1} T_{j-1/2}^n$$

$$(r_3)_j = R_{j-1/2}^{n-1} - \{ h_j^{-1} (v_j^n - v_{j-1}^n) + N^n (GV)_{j-1/2}^n - L^n X^n (FV)_{j-1/2}^n \\ - \alpha_n [(U^2)_{j-1/2}^n - (FV)_{j-1/2}^n + F_{j-1/2}^{n-1} V_{j-1/2}^n - V_{j-1/2}^{n-1} F_{j-1/2}^n] \}$$

$$(r_4)_j = S_{j-1/2}^{n-1} - \{ h_j^{-1} (T_j^n - T_{j-1}^n) - N^n (W^2)_{j-1/2}^n + (L^n X^n - \alpha_n) (UW)_{j-1/2}^n \\ - L^n (U^2)_{j-1/2}^n + N^n (GT)_{j-1/2}^n + (\alpha_n - L^n) (FT)_{j-1/2}^n - \alpha_n [-W_{j-1/2}^{n-1} U_{j-1/2}^n] \\ + U_{j-1/2}^{n-1} W_{j-1/2}^n + F_{j-1/2}^{n-1} T_{j-1/2}^n - T_{j-1/2}^{n-1} F_{j-1/2}^n \}$$

$$(r_5)_{j-1} = F_{j-1}^n - F_j^n + h_j^{-1} U_{j-1/2}^n$$

$$(r_6)_{j-1} = U_{j-1}^n - U_j^n + h_j^{-1} V_{j-1/2}^n$$

For $j = 1$, we use the wall boundary conditions and write

$$\begin{aligned} \delta F_1 &= 0 \equiv (r_1)_1 \\ \delta U_1 &= 0 = (r_2)_1 \\ \delta G_1 &= 0 = (r_3)_1 \\ \delta W_1 &= 0 = (r_4)_1 \end{aligned} \tag{4.7a}$$

and for $j = J$, we use the edge boundary conditions and write

$$\begin{aligned} \delta U_J &= 0 = (r_5)_J \\ \delta W_J &= 0 = (r_6)_J \end{aligned} \tag{4.7b}$$

The equations (4.4) for $j = 2, 3, \dots, J$ and the boundary conditions given by eq. (4.7a) for $j = 1$ and by eq. (4.7b) for $j = J$, form a linear system which is solved by the block-elimination method discussed in ref. 6.

Once the solution of the line of symmetry equations for the nose region is obtained by the above described numerical method, we then solve the system (2.41) and (2.42) subject to (2.45) by a similar procedure.

4.2 Solution of the Line of Symmetry Equations: "Zero"-Thickness Case

To solve the line of the symmetry equations (3.16) to (3.18) subject to (3.12) for the "zero"-thickness case by the Box method, we reduce them to a system of five first-order equations; we introduce new dependent variables $F(p,n)$, $G(p,n)$ and, with primes denoting differentiation with respect to n , write (3.16) to (3.18) as

$$U' = F \quad (4.8a)$$

$$W_1' = G \quad (4.8b)$$

$$\frac{\partial U}{\partial p} + \bar{V}' + a_1 U + a_2 W_1 = 0 \quad (4.8c)$$

$$F' + \beta_1^* - \bar{V}F = U \frac{\partial U}{\partial p} \quad (4.8d)$$

$$G' + \beta_2^* - \bar{V}G - U^2 - a_2 W_1^2 + a_3 UW_1 = U \frac{\partial W_1}{\partial p} \quad (4.8e)$$

We now consider one mesh rectangle in the n, p plane similar to the one shown in fig. 2 and write finite-difference approximations to (4.8) and get

$$h_j^{-1}(U_j^n - U_{j-1}^n) = F_{j-1/2}^n \quad (4.9a)$$

$$h_j^{-1}(W_j^n - W_{j-1}^n) = G_{j-1/2}^n \quad (4.9b)$$

$$h_j^{-1}(\bar{V}_j^n - \bar{V}_{j-1}^n) + (a_1^n + \alpha_n)U_{j-1/2}^n + a_2^n(W_1)_j^{n-1} = R_{j-1/2}^{n-1} \quad (4.9c)$$

$$h_j^{-1}(F_j^n - F_{j-1}^n) - (F\bar{V})_{j-1/2}^n - \frac{\alpha_n}{2}(U^2)_{j-1/2}^n = S_{j-1/2}^{n-1} \quad (4.9d)$$

$$h_j^{-1}(G_j^n - G_{j-1}^n) - (G\bar{V})_{j-1/2}^n - (U^2)_{j-1/2}^n - a_2^n(W_1)_{j-1/2}^{n-1} + (a_3^n - \alpha_n/2)(UW_1)_{j-1/2}^n \\ + \frac{\alpha_n}{2}[(W_1)_{j-1/2}^{n-1}U_{j-1/2}^n - U_{j-1/2}^{n-1}(W_1)_{j-1/2}^n] = T_{j-1/2}^{n-1} \quad (4.9e)$$

where with $\alpha_n = 2/(p_n - p_{n-1})$

$$R_{j-1/2}^{n-1} = \alpha_n U_{j-1/2}^{n-1} - [h_j^{-1}(\bar{V}_j^{n-1} - \bar{V}_{j-1}^{n-1}) + a_1^{n-1}U_{j-1/2}^{n-1} + a_2^{n-1}(W_1)_{j-1/2}^{n-1}]$$

$$S_{j-1/2}^{n-1} = -\frac{\alpha_n}{2} (U^2)_{j-1/2}^{n-1} - (\beta_1^*)^n - [h_j^{-1} (F_j^{n-1} - F_{j-1}^{n-1}) - (FV)_{j-1/2}^{n-1} + (\beta_1^*)^{n-1}]$$

$$T_{j-1/2}^{n-1} = -\frac{\alpha_n}{2} (UW_1)_{j-1/2}^{n-1} - (\beta_2^*)^n - [h_j^{-1} (G_j^{n-1} - G_{j-1}^{n-1}) - (GV)_{j-1/2}^{n-1} \\ - (U^2)_{j-1/2}^{n-1} + (\beta_2^*)^{n-1} - a_2^{n-1} (W_1^2)_{j-1/2}^{n-1} + a_3^{n-1} (UW_1)_{j-1/2}^{n-1}]$$

The resulting difference equations given by (4.9) are again nonlinear algebraic equations which are linearized by using Newton's method and are solved by the block elimination method discussed in ref. 11.

V. RESULTS

Results have been obtained and are presented for the solution of the line-of-symmetry equations for the cases of finite thickness and "zero" thickness and as a function of the angle of attack. The solution of the equations off the line of symmetry for both cases is still in progress and will be reported later.

5.1 Asymptotic Theory for Zero-Thickness Case

It is appropriate to consider some general properties of the solution before the presentation of the numerical results for the line-of-symmetry equations for the zero-thickness case. The solution starts at the stagnation point where we solve the equations given by (3.21) to (3.24) and the solution is an example of the stagnation flow studied by Howarth¹². On the windward side, p increases and the solution of (3.16) to (3.18) can be expected to approach a simple asymptotic form as $p \rightarrow \infty$. Now as $p \rightarrow \infty$, i.e. far from the nose on the windward side, it is consistent to assume that all dependent variables become independent of p and we have, with

$$\bar{V} = -\psi_0(n), \quad W_1 - U_0 = \psi'_0(n) \quad (5.1)$$

and primes denoting differentiation with respect to n ,

$$U_0'' + \psi_0 U_0' = 0 \quad (5.2)$$

$$\psi_0''' + \psi_0 \psi_0'' - (\psi_0')^2 + (2 \sin \alpha)^2 = 0 \quad (5.3)$$

where

$$\psi_0(0) = \psi'_0(0) = U_0(0) = 0 \quad (5.4a)$$

and

$$\psi'_0(\infty) = 2 \sin \alpha, \quad U_0(\infty) = \cos \alpha \quad (5.4b)$$

Thus the asymptotic solution on the windward side is essentially the same as that for a forward stagnation point in two dimensions together with a transverse boundary layer due to a uniform "cross-flow." The roles of cross-flow and mainstream seem in fact to be reversed for our problem: W is the cross-flow and is proportional to ψ'_0 when $p \gg 1$ (see (3.8b)). Suitable properties of the asymptotic solution which may be compared with numerical results include

$$U'_0(0) \rightarrow 0.5788 (2 \sin\alpha)^{1/2} \cos\alpha \quad (5.5)$$

$$W'_1(0) \rightarrow 1.2326 (2 \sin\alpha)^{3/2} + 0.5788 \cos\alpha (2 \sin\alpha)^{1/2} \quad (5.6)$$

$$\Delta_1 = \int_0^{\infty} (U_e - U_0) d\eta \rightarrow 1.016 (2 \sin\alpha)^{1/2} \cos\alpha \quad (5.7)$$

$$\Delta_2 = \int_0^{\infty} (W_e - W_1) d\eta \rightarrow \Delta_1 + 0.6479 (2 \sin\alpha)^{1/2} \quad (5.8)$$

as $p \rightarrow \infty$.

On the leeward side, we integrate in the direction of p decreasing and once we are past the nose, so that p is negative, either $\partial U / \partial n$ vanishes at some finite value $p_s(\alpha)$ of p or it reaches a (negative) maximum (see fig. 5) and then decreases again. In the first case a singularity develops at $p = p_s$ (see ref. 12) and in the second the solution can be continued to all negative values of p and there is a consistent asymptotic form which it approaches. This form is in two parts. Near the body ($n \sim 1$) we write, for large negative values of p

$$\bar{V} = -\Phi'_0(n), \quad W_1 + U_0 = \Phi'_0(n) \quad (5.9)$$

so that from (3.8b) $-\Phi'_0$ gives the cross-flow velocity W . Then Φ'_0 satisfies the same differential equations as ψ'_0 , and U_0 satisfies (5.2) and (5.3). The boundary conditions are also the same as (5.4) but some comment is needed about $\Phi'_0(\infty)$. According to (3.14b) $\Phi'_0(\infty)$ should be equal to $-2 \sin\alpha$ but it is well known that (5.2) and (5.3) does not then have a solution. The solution of this apparent contradiction is to be found in Proudman and Johnson's study of the unsteady boundary layer near the rear stagnation point of a two-dimensional bluff body¹³. This asymptotic solution may easily be adapted to our problem with p playing the role of time. The appropriate boundary condition to complete the specification of (5.10), (5.11) is then

$$\Phi'_0(\infty) = +2 \sin\alpha \quad (5.10)$$

which means that near the body $W/\cos\theta > 0$ and so the boundary layer behaves on the leeside and windward sides in essentially the same way - fluid is being carried along the line of symmetry and nearby the streamlines are curved away from it so that fluid is also moving out of the symmetry plane. Also apart from the obvious change in sign of $U'_0(0)$, the properties (5.5) to (5.8) are the same on the leeward side.

As $n \rightarrow \infty$, $U_0 \rightarrow -\cos\alpha$ and $W_1 + U_0 \rightarrow 2 \sin\alpha$ whereas it should be $\rightarrow -2 \sin\alpha$. The adjustment of this boundary condition takes place over a length scale in n which is an exponentially large function of p and in which viscous forces can be neglected and U_0 may be regarded as sensibly constant. We write

$$\xi = n \exp(2p \tan\alpha) \quad (5.11)$$

$$V = 2 \sin\alpha e^{-2p \tan\alpha} F(\xi), \quad W_1 + U_0 = -2 \sin\alpha F'(\xi) \quad (5.12)$$

where primes now denote differentiation with respect to ξ . On substituting into (3.16), (3.18) we obtain

$$(F - \xi)F'' = F'^2 - 1 \quad (5.13)$$

with boundary conditions

$$F' \rightarrow 1 \quad \text{as } \xi \rightarrow \infty, \quad F(0) = 0 \quad (5.14)$$

to match up with the prescribed mainstream conditions and with the inner solution (5.9) valid when $n \sim 1$ and hence when $\xi \ll 1$. Specifically we notice that $F(0) = 0$ implies $F'(0) = -1$. The solution of (5.13) is

$$F = \xi - \frac{2}{c} (1 - e^{-\xi c}) \quad (5.15)$$

where c is a constant dependent in some way on the history of the boundary layer for finite p and determined by matching with the numerical computation. Reference may be made to Proudman and Johnson's paper for details of the arguments leading to the choice of the scaling law (5.13) and discussion of various alternatives.

A possible interpretation of this result is as follows. There is a curve C on the paraboloid, symmetric with respect to the leeward line of symmetry ℓ and open as $p \rightarrow -\infty$ on which the crossflow velocity is zero. The limiting

streamlines of the boundary layer (or skin-friction lines) all start from the stagnation point S_0 and two of them are the windward ℓ_n and leeward ℓ_l lines of symmetry. Limiting streamlines initially inclined close to ℓ_n move away from it as S increases ultimately asymptoting to C when $\theta \approx 106^\circ$, corresponding to the separation angle of a circular cylinder. The other limiting streamlines also move away from the ℓ_w and, once the nose is passed, towards the ℓ_l but eventually they must cross C when they turn back towards ℓ_w but never reaching it of course. Instead they either asymptote to C from the other side as $p \rightarrow -\infty$ or generate a separation line at finite values of p .

A surface Σ can also be defined, standing on C , on which the cross-velocity is zero. One of its principal properties is that its height increases exponentially as $p \rightarrow -\infty$. Streamlines in the boundary layer initially above the limiting streamlines in the neighborhood of ℓ_w are directed away from the paraboloid and this line and pass above Σ . Other streamlines also move initially towards ℓ_l and away from the body but once they cross Σ the cross-flow velocity is reversed and they begin to move back towards ℓ_w . Further if they are sufficiently near the body their outward motion is temporarily also reversed, but not at Σ . Eventually they will again move away from the body and are likely to end up asymptoting the inside of Σ or some separation surface. Thus, the general shape of the streamlines is spiral although it is unlikely that more than one revolution is completed. Complications can arise if the streamlines form internal envelopes but evidence is lacking in support of these possibilities.

5.2 The Two-Dimensional Airfoil

The equivalent results for the boundary layer near the nose of a two-dimensional bluff body are obtained in a more straightforward way than for bodies of revolution, but the fundamental equations take a little more space to derive because a suitable reference is lacking. We begin by considering the inviscid flow past an ellipse at an incidence α with circulation $2\pi k$ (neglected in Chapter 2). We define (x,y) as Cartesian coordinates with origin O at the center of the ellipse Ox along the major axis and Oy along the minor axis. Then, according to complex variable theory, the complex potential for attached flow is

$$w = \zeta e^{-i} + \zeta^{-1} e^i + i\kappa \log \zeta, \quad z = \zeta + \frac{c^2}{\zeta} \quad (5.16)$$

where $w = \phi + i\psi$, ψ is the stream function of the flow and $z = x + iy$. In this solution the circle $\zeta = e^{-i\theta}$ corresponds to the ellipse $x = -(1 + c^2) \cos \theta$, $y = (1 - c^2) \sin \theta$ and nondimensional variables are used so that the fluid speed at infinity is unity and the major axis of the ellipse is $2(1 + c^2)$.

We are specifically interested in the neighborhood of the nose (i.e. $x = -(1 + c^2)$, $y = 0$) when $0 < (1 - c^2) \ll 1$. Let us write $1 - c^2 = 2t$, so that t is the (small) thickness ratio of the ellipse and

$$\theta = -t\xi \quad (5.17)$$

Near the nose $x + 2 = t^2 \xi^2$, $y = 2t^2 \xi$ on the ellipse, and the velocity of slip round the ellipse is

$$u_e(\xi) = \frac{\xi - \beta}{\sqrt{\xi^2 + 1}} \quad (5.18)$$

when $\xi = 0(1)$, where $\beta t = (2\alpha - \kappa)$. From thin airfoil theory we may take $\kappa = \alpha$ and we shall assume $\beta > 0$.

The boundary-layer equations needed to reduce this slip velocity to zero at the ellipse are now easily obtained. We suppose, that the normal distance Y from the ellipse and the streamfunction ψ are scaled with $t\sqrt{2v}$ where v is the kinematic viscosity and arc length X on the ellipse with $2t^2$ so that

$$X = \frac{1}{2} \xi \sqrt{1 + \xi^2} + \frac{1}{2} \sinh^{-1} \xi \quad (5.19)$$

With external velocity distribution given by (5.18) and with surface distance given by (5.19), the governing boundary-layer equations are solved by the Box scheme described in ref.11. The solution procedure starts at $\bar{X} = 0$ with $\xi = \beta$ where

$$\bar{X} = X - X_0$$

with X_0 computed from (5.19) by letting $\xi = \beta$. The integration, which starts as the Hiemenz stagnation point flow, tends to the Blasius form on the pressure side of the airfoil as $X \rightarrow +\infty$. On the suction side X

decreases and u_e reaches a negative minimum value of $-(1 + \beta^2)$ at $\xi = -1/\beta$, i.e. just past the nose, and thereafter increases again to -1 as $X \rightarrow -\infty$ (see fig. 3). Provided, therefore, that the integration does not break down at a finite value of X , the solution on the suction side also takes on the Blasius form as $X \rightarrow -\infty$. However, if the pressure gradient parameter β is strong enough, the solutions indicate separation. This occurs if

$$\beta > \beta^* = 1.155 \quad (5.20)$$

For these values of β , the solution is terminated at the separation point \bar{X}_s shown in figure 4 as a function of β . It is interesting to compare this criterion for the onset of separation with the experimental data provided by Gault². For the NACA 663-018 airfoil with a leading-edge radius of curvature corresponding to $t = 0.20$, incipient separation occurs when $\alpha = 7^\circ$, i.e. $\beta = 0.61$. The most likely explanation for the discrepancy with (5.20) is that this airfoil is not exactly parabolic near the nose. Thus, if we define β by the position of the forward stagnation point, $\beta = 1$ at $\alpha = 7^\circ$ and if we define it by the pressure minimum $\beta = 1.45$. A somewhat similar situation occurs with the modified NACA-0010 airfoil. Here $t = 0.16$ and the corresponding values of β are 0.43, 0.6 and 1.0.

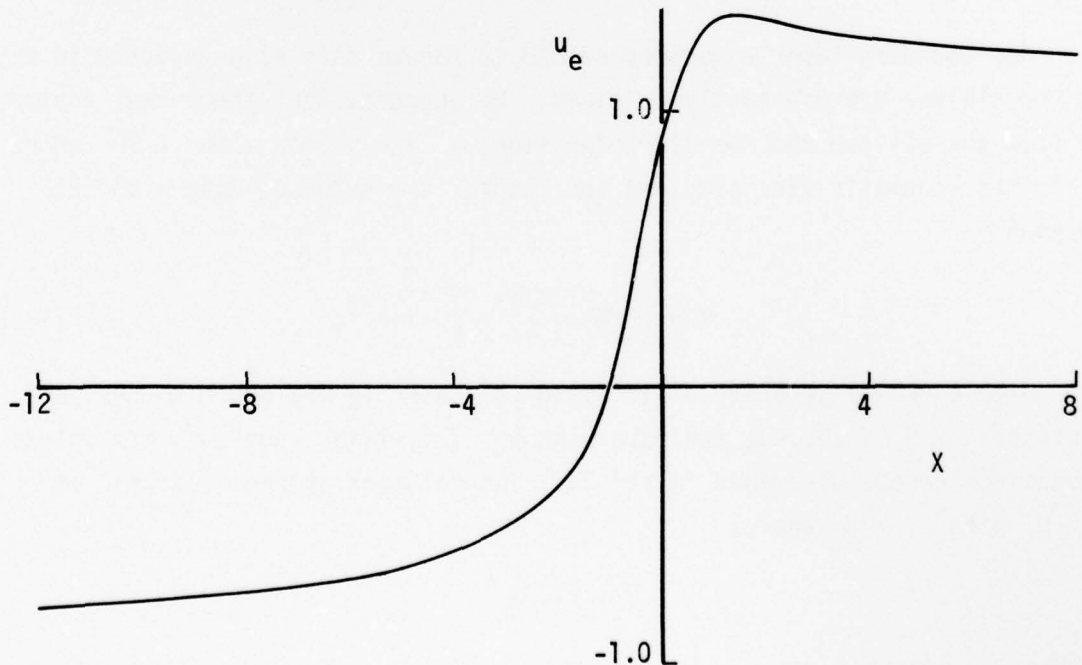


Figure 3. Variation of u_e with X for $\beta = 0.9$.

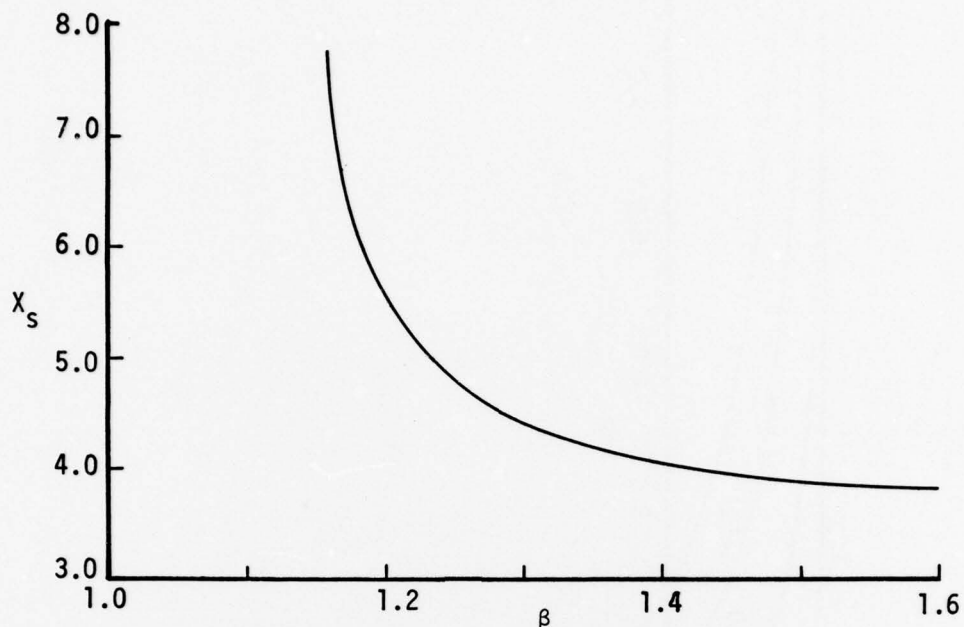


Figure 4. Variation of separation point with β .

5.3 Numerical Results for the Line of Symmetry Flow

The numerical results obtained here are in good agreement with the earlier results for finite thickness by Wang⁹ and in Hirsh and Cebeci¹⁴ and for "zero"-thickness by the asymptotic theory of Section 5.1. Figures 5 and 6 show, for the zero-thickness case, the variation of the longitudinal and transverse components of wall shear, namely $U'_0(0)$ and $W'_0(0)$ with p for various angles of attack. On the leeward side the longitudinal component of the wall shear develops a maximum and a minimum for moderate but not too large values of α . As α increases, the peak and dip in the wall shear on the leeward side near the nose becomes more pronounced and at $\alpha = 41^\circ$, this component of the wall shear actually vanishes at $p_s = -1.38$, terminating the computation. At larger values of α , it vanishes nearer the nose and indeed formally we may expect that as $\alpha \rightarrow 90^\circ$, separation takes place at $p = 0$. The variation of p_s with α is shown in figure 7. Also shown in figs. 5 and 6 are the asymptotic values for $U'_0(0)$, $W'_0(0)$ and $\alpha = 30^\circ$ both on the windward and leeward sides computed from (69) et seq. It is clear that the results are consistent.

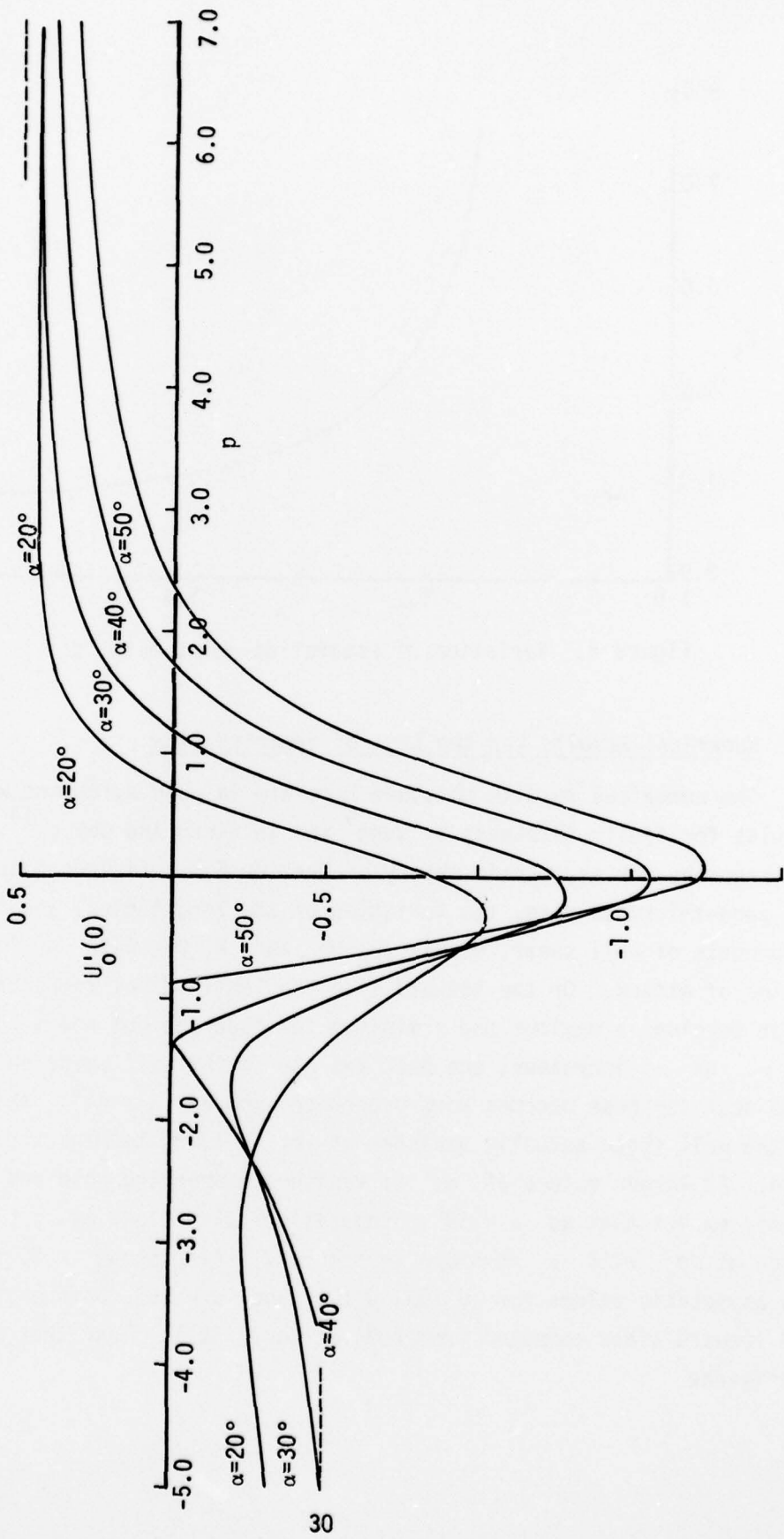


Figure 5. Variation of the longitudinal component of wall shear, $U'_0(0)$ for paraboloids of zero thickness ratio with p for various α . The dashed lines indicate the asymptotic results for $\alpha = 30^\circ$.

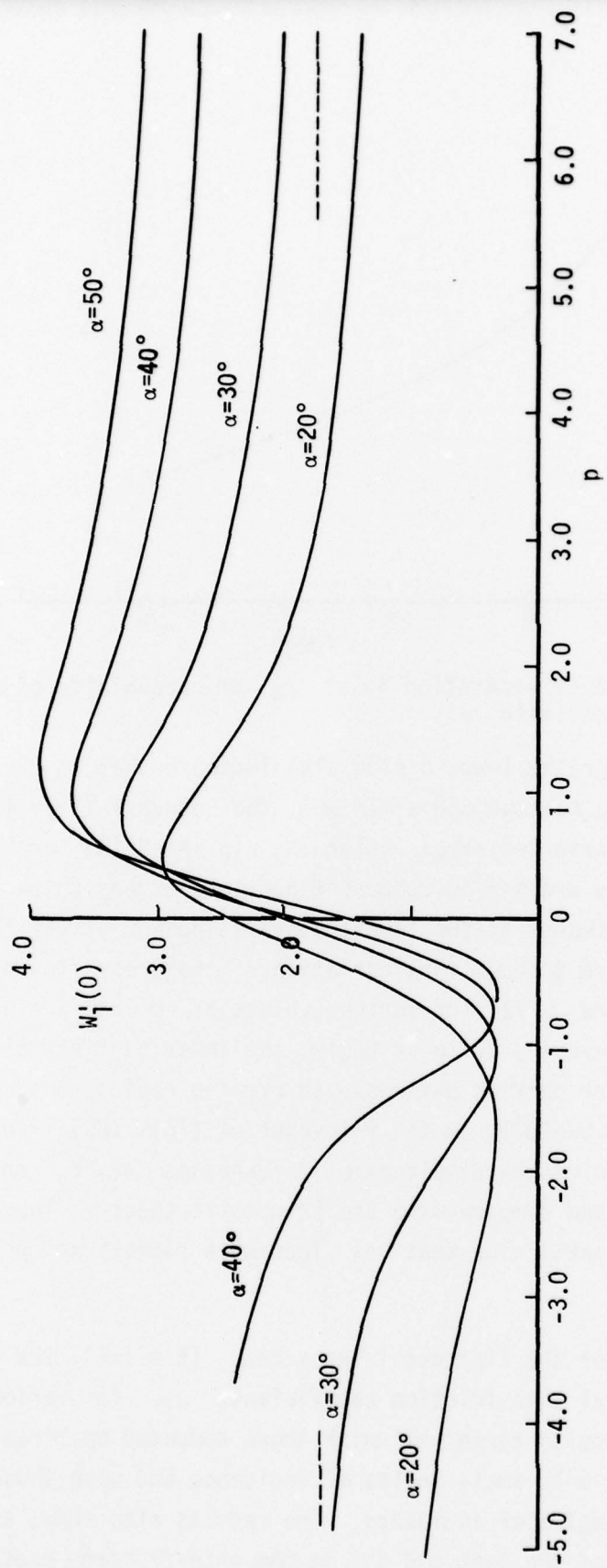


Figure 6. Variation of the transverse component of wall shear $W_l'(0)$ for paraboloids of zero thickness ratio with p for various α . The dashed lines indicate the asymptotic results for $\alpha = 30^\circ$.

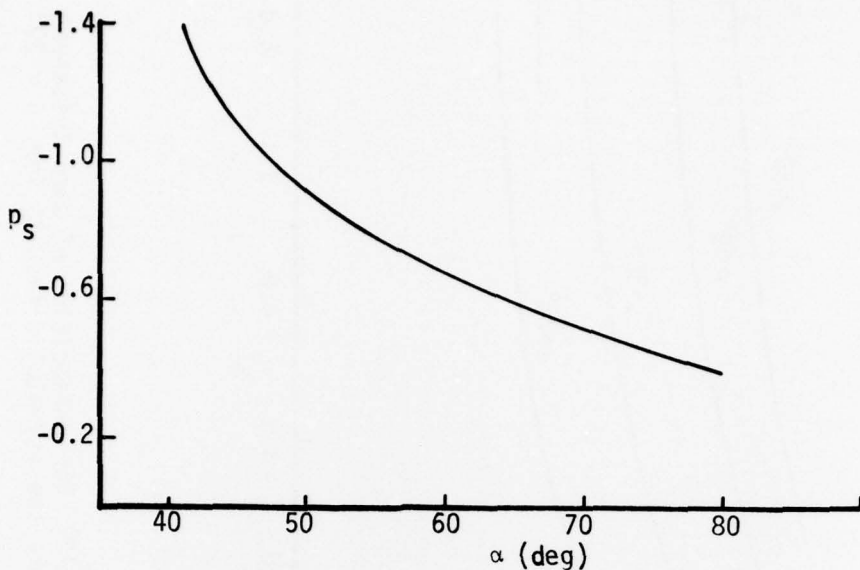


Figure 7. The variation of separation point p_s on paraboloids of zero thickness ratio with α .

The calculations for the leeward side also indicate that in the region where $U'_0(0)$ exhibits a maximum and a minimum, the boundary-layer thicknesses of U_0 and W_1 are nearly the same. After the dip in $U'_0(0)$ or rise in $W'_1(0)$ (see fig. 6), the cross-flow component develops a very thick boundary layer; the boundary thickness of the longitudinal component of the flow remains nearly unchanged. Figure 8 shows that variation of the cross-flow profile (3.8) on the leeward side S_w/Z for various values of p at $\alpha = 30^\circ$. The double structure is developing quite strongly, the inner part asymptotting to the limit (74), the outer part is obviously thickening rapidly but p is too small for us to comment usefully on the relevance of (76), (80). In figure 9 we display the variation of the displacement thicknesses Δ_1, Δ_2 on the windward and leeward sides and compare with the asymptotic theory. The agreement is good and we note in particular that Δ_2 increases rapidly as p decreases below p_s .

Figure 10 shows, for the finite-thickness case ($t = 1/4$), the variation of the longitudinal local skin-friction coefficient, c_f , for various angles of incidence. These results agree well with those computed by Hirsh and Cebeci¹⁴ who considered only small angles of incidence and with those of Wang⁹ who considered larger angles of incidence. The results also show, as in the zero-thickness case, that the peak and dip in the skin-friction coefficient on

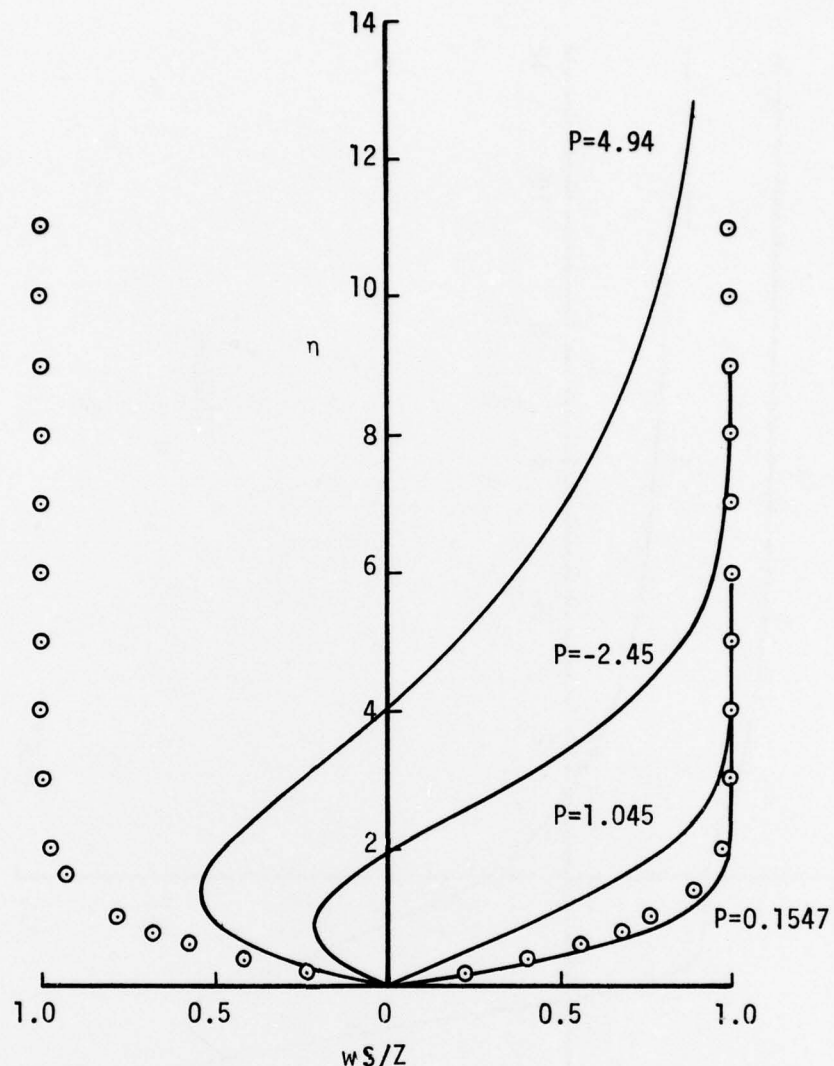


Figure 8. The profiles of the cross-flow velocity w at $\alpha = 30^\circ$ for various values of p : - o - o - o - o are the asymptotic forms, windward to the right and leeward to the left. The dependence of w on Z/S has been scaled out.

the leeward side near the nose becomes more pronounced with increasing angle of incidence and, the local skin-friction vanishes at approximately 42 degrees, indicating separation. It is remarkable that this result is in excellent agreement with the one computed by using the zero-thickness case. Further comparisons and calculations will be made when the solutions are extended off the line of symmetry for both zero and finite-thickness cases.

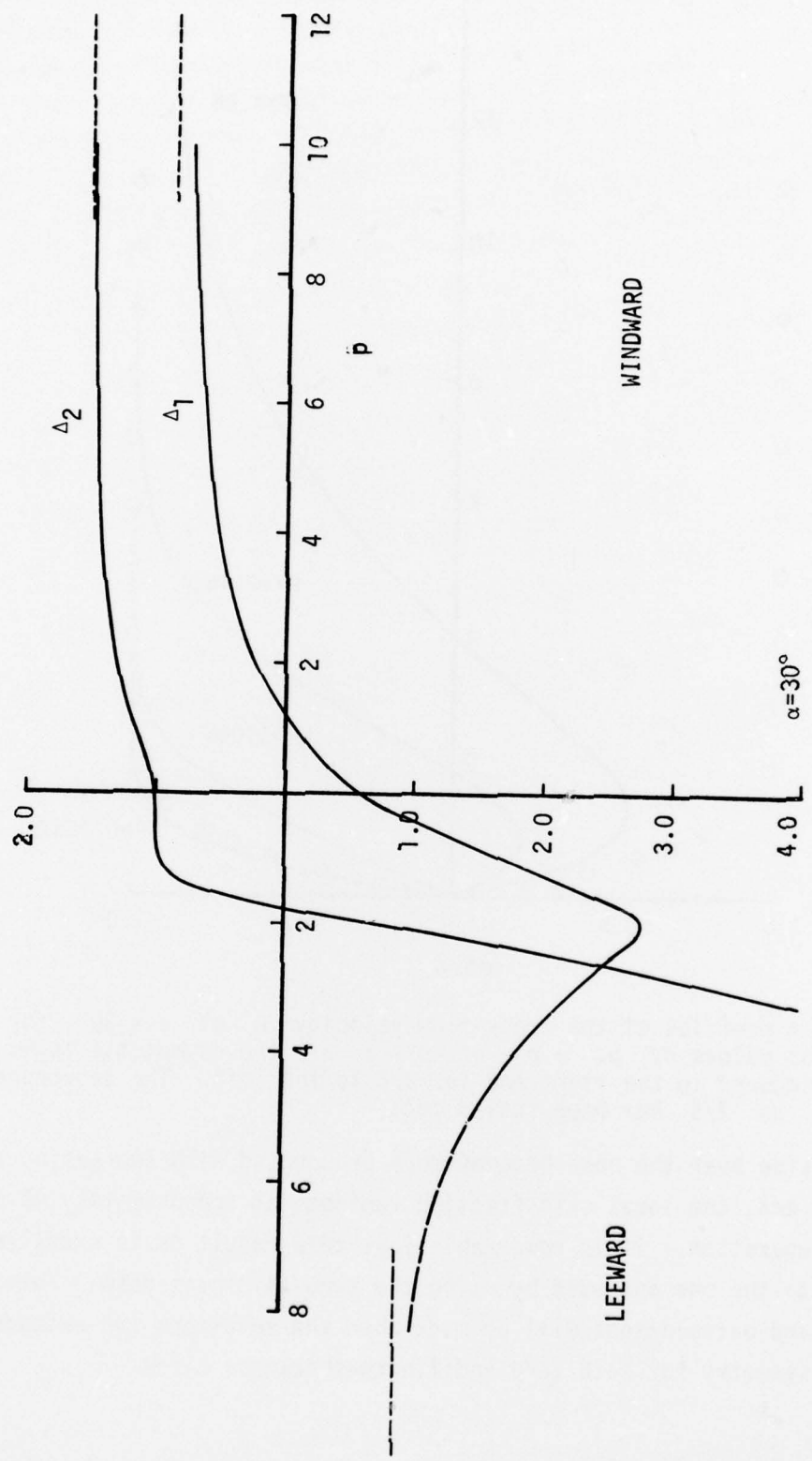


Figure 9. The variation of Δ_1 , Δ_2 for paraboloids of zero thickness with p for $\alpha = 30^\circ$. The dashed lines are the asymptotic results.

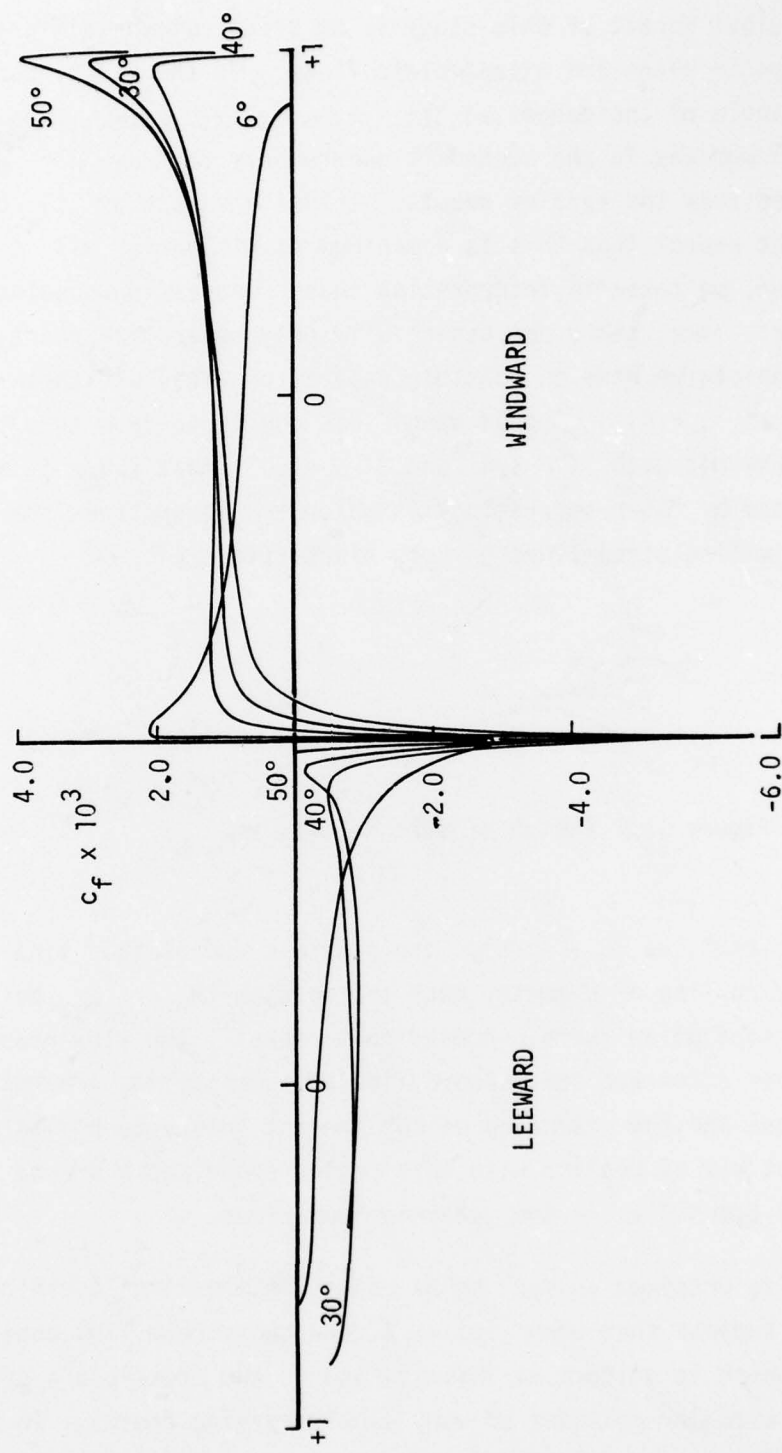


Figure 10. The variation of the longitudinal local skin-friction coefficient, c_f , with axial distance from the nose ($x = -1$) for a paraboloid of thickness ratio $1/4$ and various angles of incidence.

VI. DISCUSSION

The principal result of this study is to bring out the difference between nose-separation in plane and axisymmetric flows. In the first, separation occurs at an angle of incidence $\approx 1.16t$ where t is a representative thickness of the airfoil whereas in the second it occurs only for $\alpha > 41^\circ$ when $t \ll 1$. Indeed from the earlier results at finite values of t , due to Wang¹⁵ we might expect that this is a minimum condition for all t . Care must, of course, be taken in interpreting these contrasting conclusions. In two-dimensional flows, there are essentially only separation points whereas in three dimensions we have to consider separation lines and these may occur near the nose at $\alpha < 41^\circ$. Indeed Wang¹⁵ has concluded from this study of the prolate spheroid with $t = 1/4$ and $\alpha = 30^\circ$ that there is a phenomenon which he denoted by "open separation" in which the separation line is an envelope of limiting streamlines on both sides (fig. 11).



Figure 11. Sketch of open separation.

It is possible that, as $\alpha \rightarrow \alpha_s(t)$, the upstream end of this line moves on to the leeward line of symmetry near the nose, with $\alpha > \alpha_s$ being the condition for separation there. According to Wang¹⁵, the flow properties between open separation and the leeward line of symmetry are not fully understood at present and the extension of the present theory to points off ℓ may be the simplest way of dealing with this region since there are no irregularities or small quantities in the governing equations.

The results obtained so far raise some interesting questions. For one might suppose that when $|p| \gg 1$, the mainstream flow consists of a component, which is uniform at infinity and in the cross-plane of the body, moving past a circular cylinder of very slowly varying radius. In addition, there is a uniform component of velocity perpendicular to this plane. Very

like the yawed-infinite-wing problem in fact! The windward asymptotic solution supports this view. Hence, in view of the independence principle¹⁶, we should be able to integrate the cross-flow equation (for w) independently of those for when $|p| \gg 1$ and since these lead to separation at $\theta = 104^\circ$ (ref. 11) this point could give the asymptotic position of Wang's open-separation line when $\alpha < 41^\circ$ and $|p| \rightarrow \infty$.

However, we are inclined to be cautious at present. For the singularity in the cross flow at separation prevents the solution from being continued to larger values of θ whereas we know from the leeward line of symmetry solution that one can be found at $\theta = \pi$ for all p . Further the use made of the Proudman-Johnson theory in Section 5.1 suggests that there is an analogy between the role of p in the present theory and of t in unsteady two-dimensional theory. There has been some controversy in the past about the values of unsteady boundary layers on the circular cylinder, particularly as to whether they can develop singularities at finite times but it now seems clear (ref. 17) that they remain smooth, although growing exponentially near the rear-stagnation point. Is the same situation true here? The main differences occur near the body when $n \sim 1$ and $u_0 \neq 1$ so that the analogy fails and if $p \sim 1$ when separation might take place on ℓ if α is large enough. If the analogy is nevertheless qualitatively acceptable, the conclusion is that the flow is smooth over the nose region for all finite p but that beyond a certain line, roughly given by the reversal of the cross-flow component of the skin friction the cross-flow boundary layer increases rapidly in thickness with p . On the other hand, the failure of the analogy when $n \sim 1$ may permit the existence of an open separation line or even of a separation tongue one end asymptotting to $\theta = 104^\circ$ as $p^2 \rightarrow \infty$ and the other to a larger value of θ .

This discussion seems to have relevance to yawed wings which are not axisymmetric. The independence principle applies here too and suggests that the boundary solution must be terminated at the separation of the cross flow. We now wonder whether this is necessarily the case. Provided separation of the boundary-layer component in the spanwise direction has not occurred near the upstream wing-tip and the distance from the tip is finite, it may be possible to carry out the integration beyond the cross-flow reversal right up to the trailing edge. Of course, the cross-flow boundary layer then increases

in thickness rapidly with p but the boundary-layer assumptions are still valid so that we would be able, without any contradictions, to advance the integration beyond the separation line in the form it is understood at present. The avoidance of separation near the wing-tip might, however, not be easy in practice, especially since an unyawed wing corresponds essentially to setting $\alpha = 90^\circ$.

A final question raised by these studies concerns the flow near the nose of smooth three-dimensional bodies, for example thin ellipsoids at incidence. If the mainstream is symmetric about a plane of symmetry of the ellipsoid, then the boundary layer on one of the lines of symmetry can be computed using similar methods to those of this report and indeed our present results can be regarded as limiting cases accordingly as the cross-section of the ellipsoid is a circle (Section 5.1) or has an infinite major axis (Section 5.2). Presumably the critical angle for nose separation varies from 41° to 0° as the eccentricity of the cross-section increases from 0 to 1. It would be interesting to know how close we must be to a two-dimensional form before separation occurs at relatively small angles of attack and indeed what is the effect of an asymmetric mainstream so that there is no line of symmetry along which the integration can be carried out independently of the rest of the flow field.

VII. REFERENCES

1. Jones, B.M.: Stalling. J.R. Aero. Soc., Vol. 38, pp. 753-770, 1934.
2. Gault, D.E.: An Experimental Investigation of Regions of Separated Laminar Flow. NACA Tech. Note, No. 3505, 1955.
3. Tani, I.: Low-Speed Flows Involving Bubble Separations. Prog. in Aero. Sci., Vol. 5, pp. 70-103, 1964.
4. Gaster, M.: The Structure and Behavior of Laminar Separation Bubbles. Separated Flows, Part 2, AGARD Conf. Proc. No. 4, p. 819, 1966.
5. Briley, W.R. and McDonald, H.: Prediction of Incompressible Separation Bubbles. J. Fluid Mech., Vol. 6, pp. 631-656, 1955.
6. Goldstein, S.: On Laminar Boundary-Layer Flow Near a Position of Separation. Quart. J. Mech. Appl. Math., Vol. 1, p. 43, 1948.
7. Smith, F.T.: The Laminar Separation of an Incompressible Fluid Streaming Past a Smooth Surface. Proc. Roy. Soc., Lond. A, Vol. 356, pp. 443-464, 1977.
8. Wang, K.C.: Separation of Three-Dimensional Flow in Reviews in Viscous Flow. Proceedings of the Lockheed-Georgia Co. Viscous Flow Symposium, pp. 341-414, June 1976.
9. Wang, K.C.: Three-Dimensional Boundary Layer Near the Plane of Symmetry of a Spheroid at Incidence. J. Fluid Mech., Vol. 43, p. 187-209, 1970.
10. Wang, K.C.: Boundary Layer Over a Blunt Body at Low Incidence with Circumferential Reversed Flow. J. Fluid Mech., Vol. 72, pp. 49-65, 1975.
11. Cebeci, T. and Bradshaw, P.: Momentum Transfer in Boundary Layers. McGraw-Hill/Hemisphere Publishing Co., Washington, D.C., 1977.
12. Brown, S.N. and Stewartson, K.: Laminar Separation. Ann. Rev. Fluid Mech., Vol. 1, pp. 45-72, 1969.
13. Proudman, I. and Johnson, K.: Boundary-Layer Growth Near a Rear Stagnation Point. J. Fluid Mech., Vol. 14, pp. 161-168, 1962.

14. Hirsh, R.S. and Cebeci, T.: Calculation of Three-Dimensional Boundary Layers with Negative Cross Flow on Bodies of Revolution. AIAA Paper 77-683, 1977.
15. Wang, K.C.: Boundary Layer Over a Blunt Body at High Incidence With an Open-Type of Separation. Proc. Roy. Soc., London, A340, pp. 33-55, 1974.
16. Jones, R.T.: Effects of Sweepback on Boundary Layer and Separation. N.A.C.A. TR 884, 1947.
17. Cebeci, T.: On the Problem of Laminar Flow Over a Circular Cylinder Started Impulsively from Rest. In press. J. of Computational Physics, 1978.

Unclassified

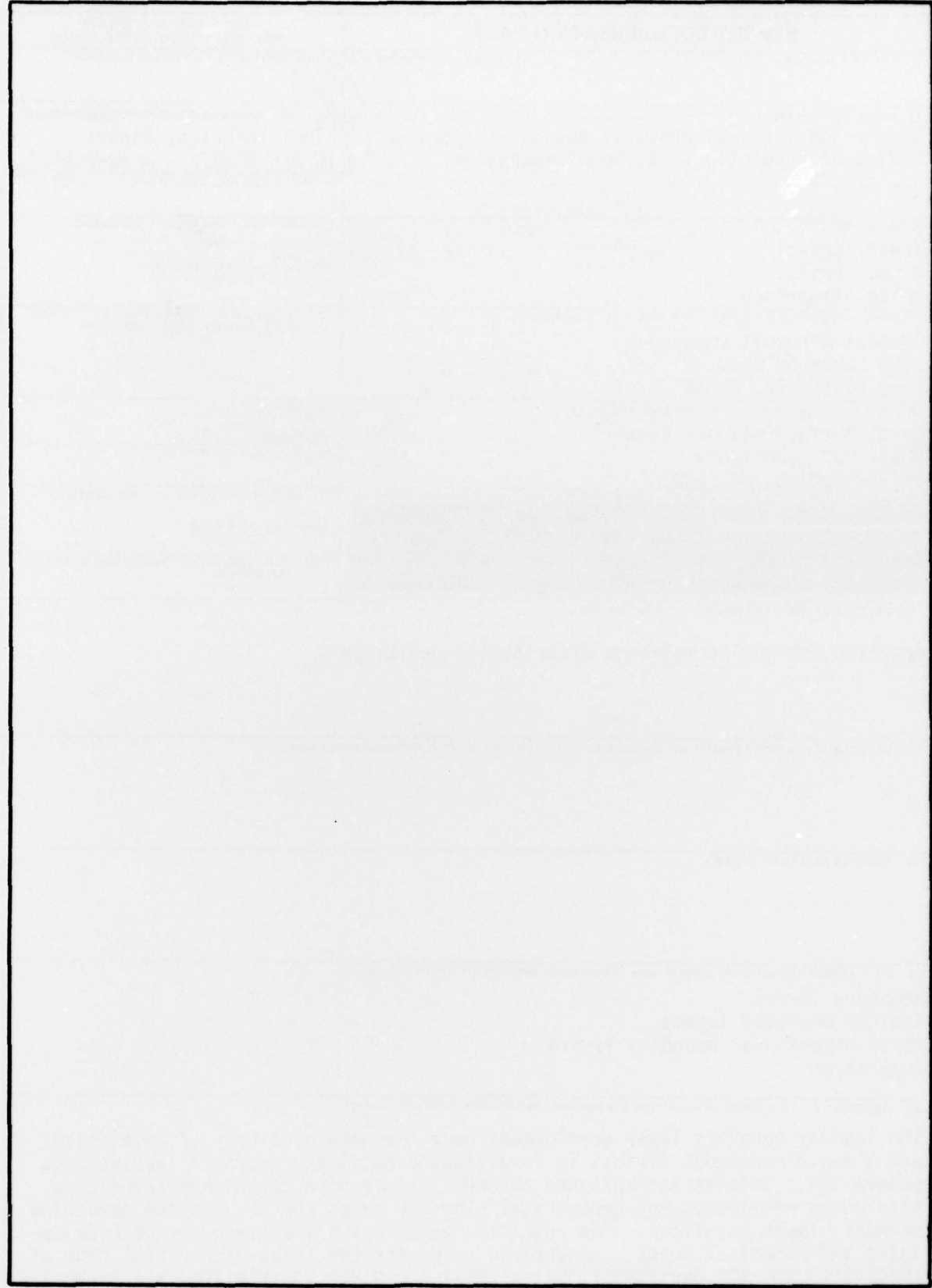
SECURITY CLASSIFICATION OF THIS PAGE (When Data Entered)

REPORT DOCUMENTATION PAGE		READ INSTRUCTIONS BEFORE COMPLETING FORM
1. REPORT NUMBER	2. GOVT ACCESSION NO.	3. RECIPIENT'S CATALOG NUMBER
4. TITLE (and Subtitle) Studies on Three-Dimensional Boundary Layers on Bodies of Revolution. I. Nose Separation.		9 TYPE OF REPORT & PERIOD COVERED Final Technical Report 18 April 1977 - August 1978
7. AUTHOR(S) Tuncer/Cebeci, A. K. Khattab Keith Stewartson		6. PERFORMING ORG. REPORT NUMBER 14 MDC-J7985 15 N60921-77-C-0096
8. CONTRACT OR GRANT NUMBER(S)		10. PROGRAM ELEMENT, PROJECT, TASK AREA & WORK UNIT NUMBERS 12 46P. 1
9. PERFORMING ORGANIZATION NAME AND ADDRESS Douglas Aircraft Company 3855 Lakewood Blvd. Long Beach, Ca. 90846		11. REPORT DATE 11 August 1978
11. CONTROLLING OFFICE NAME AND ADDRESS Naval Surface Weapons Center White Oak Laboratory Silver Spring, Md. 20910		13. NUMBER OF PAGES 42
14. MONITORING AGENCY NAME & ADDRESS (if different from Controlling Office)		15. SECURITY CLASS. (of this report) Unclassified
16. DISTRIBUTION STATEMENT (of this Report) Approved for public release; distribution unlimited		15a. DECLASSIFICATION/DOWNGRADING SCHEDULE
17. DISTRIBUTION STATEMENT (of the abstract entered in Block 20, if different from Report)		
18. SUPPLEMENTARY NOTES		
19. KEY WORDS (Continue on reverse side if necessary and identify by block number) boundary layers laminar boundary layers three-dimensional boundary layers separation		
20. ABSTRACT (Continue on reverse side if necessary and identify by block number) The laminar boundary-layer development near the nose of a body of revolution and a two-dimensional airfoil is investigated until the onset of leading-edge separation. This is accomplished through the use of a coordinate transformation which eliminates any geometrical singularity at the nose in the governing boundary-layer equations. The resulting equations are examined by both asymptotic and numerical means. Comparable cases for the three-dimensional body of revolution and the two-dimensional airfoil are given and similarities as well as differences are discussed.		

DD FORM 1 JAN 73 1473 EDITION OF 1 NOV 65 IS OBSOLETE
S/N 0102-014-6601Unclassified
SECURITY CLASSIFICATION OF THIS PAGE (When Data Entered) JB

116 400

SECURITY CLASSIFICATION OF THIS PAGE(When Data Entered)



SECURITY CLASSIFICATION OF THIS PAGE(When Data Entered)